Reprinted: 23-05-2001
Website: www.shipmotions.nl

Report 288, April 1970,
Delft University of Technology,
Ship Hydromechanics Laboratory,
Mekelweg 2, 2628 CD Delft,
The Netherlands.

Prediction of Ship Manoeuvrability Making Use of Model Tests

G. van Leeuwen and J.M.J. Journée

Delft University of Technology

Summary

Static sway- and oscillatory yawing tests with a 1:55 model of the 50.000 DWT tanker "British Bombardier" are discussed. The principal purpose of these tests was to determine the coefficients of a non-linear mathematical model to predict a number of standard manoeuvres, which were earlier performed with the full-scale ship. The results of these full-scale manoeuvres are described in reference Clarke (1965). The mathematical model chosen is based on the Abkowitz Taylor-expansion of the hydrodynamic forces and moments see Abkowitz (1964). However, there is a principal difference with respect to the variables involved, which enables a more correct description of some non-linear phenomena. Comparison of the predicted manoeuvres with the corresponding full-scale data shows a rather good agreement. For comparison purposes also some experiments have been performed with a small model of the same tanker ($a = 100$). However it is found that scale effects, due to the very low Reynolds number have a considerable influence on the hydrodynamic derivatives. Some interesting additional figures are given, showing the contributions of each term of the mathematical model during a turning circle manoeuvre while also the change of the stability roots during this manoeuvre is plotted.

1 Introduction

At the Delft Shipbuilding Laboratory model tests are performed to determine the coefficients of a non-linear mathematical model, which describes the still water manoeuvrability properties of a ship. Two types of tests are performed: firstly the static towing tests with a constant drift- and rudder angle and secondly oscillation tests to determine the added mass effect in the swaying motions and the hydrodynamic derivatives of the yawing motion.

The principal purpose of the tests is to obtain information on the possibility to predict the principal manoeuvres of a ship, using an adequate mathematical model and model

experiments to determine the coefficients of this model. For comparison purposes also Clarke (1965) performs full-scale trials.
The model experiments have been performed at four different initial speed conditions, corresponding with a constant propeller power each. Originally the results of these four sets of tests have been kept separated because it was assumed that some of the non-dimensional coefficients could change with the Froude number, based on the initial speed. In that case a set of coefficients, which would be different for each initial speed, would have been found. Van Leeuwen (1969c) gives the results of this tentative analysis.
During the analysis of the experimental data, it was found that the principal differences between some of the non-dimensional coefficients could be described effectively by considering the local water velocity near the rudder. In this way the apparent Froude-effect in these coefficients rather could be called a "power-effect" while the differences in the other coefficients were not considered significant, in view of both the available information and the accuracy of the measurements.
It is not to be expected however, that this method of describing the phenomena mentioned above will hold for other ships. Especially when the Froude number becomes high, e.g. 0.30 or higher, it is not very likely that there will be no real Froude-effect in some hydrodynamic derivatives, if they are compared with the corresponding values found at a Froude number of 0.10 e.g.

Provided a certain mathematical model has been adopted, there are several methods to determine the coefficients of such a model by model tests. The main problem is to find out how far it is allowed to uncouple the three motions in the horizontal plane. Of course, during an actual manoeuvre the motions are always coupled and even if the mathematical model contains terms which are meant to describe the cross-coupling effects, one is not sure about the way these effects have to be determined. The most convenient method might be to perform free running model tests and find the coefficients of the mathematical model by analysing the data concerning position and course of a number of representative manoeuvres. In that case all variables remain coupled in the natural way. In general however too less room is available for these kinds of manoeuvres, so that one is pressed to find an acceptable alternative. In this respect the forced horizontal oscillation test provides an alternative solution. On the other hand amongst others, the problem of uncoupling the motions as mentioned above is introduced. Another practical problem is to choose the right combinations of oscillator frequencies and amplitudes. Considering an actual oscillatory motion, due to the harmonic motion of the rudder, it is found that the combinations of frequencies and amplitudes involved in these motions, cannot easily be simulated by horizontal oscillation tests. This is because the actual range of amplitudes is of the magnitude of one half to many ship lengths. In most towing tanks sufficient width is not available in this respect. These problems are considered in greater detail in by Van Leeuwen (1969a).
The conclusion is that most horizontal oscillation tests involve an unnatural relation between amplitudes and frequencies. In other words the ratios of velocity and acceleration amplitudes are quite different from the actual values. Apparently this is no problem, because most of the mathematical models which are now in use do not contain any cross-coupling terms between velocities and accelerations. This does not imply however that such cross-coupling effects could not be introduced, if the range of ratios of these variables is extended too far.

Finally, some remarks considering the mathematical model.
In the course of the years a lot of studies have been devoted to this subject starting with Davidson and Schiff (1946), who described a model based on the linear equations of motion. This set of equations - which originally involves three equations describing the surging

swaying and yawing motion - has been used by several authors, though unfortunately omitting the surge equation. Abkowitz (1964) has proposed one of the most extended non-linear mathematical models. In this model the hydrodynamic part of the forces is expanded into a Taylor series of the variables concerned. This principle is very useful, particularly if the constants of the model are to be determined by the analysis of forced model tests, because all imaginable hydrodynamic effects in principle can be described in this way. An important question involved in this Taylor-expansion is up to which degree it has to be extended to be sure that the principal non-linear hydrodynamic effects are described correctly. On the other hand it is questioned to what extend it is necessary to retain a great number of terms in such a model for a reasonable accurate description of manoeuvres, even if the separate hydrodynamic effects involved can be measured with forced model tests. In other words it is suggested that, on the ground that during an actual manoeuvre the ratios of the variables satisfy just one relation, it might be possible to describe the joint effect of a number of terms by one term only. In this way a quite simpler mathematical model would arise, the coefficients of which had to be considered functions of the coefficients of the original model. Van Leeuwen (1970) describes some simple non-linear models based on these grounds.
A disadvantage of such simplified mathematical models is that its coefficients cannot be determined by uncoupling the three motions, which means that they can only be derived from free running tests, either full-scale or model tests. For practical purposes however, such as simulation studies and automatic piloting, these simplified non-linear models can be applied successfully.

The principle of the mathematical model used for the present model tests is, apart from some details, the same as has been used by Abkowitz. The way upon which Abkowitz handles the influence of a change of the forward speed however brings about that no insight is gained into the physical background of this influence.

In this paper, the hypothesis is used that if the motions are similar, regarding velocities and accelerations, the principal hydrodynamic forces on the hull are proportional with the square of the instantaneous forward speed. For the forces, which mainly depend on the effective angle of attack of the rudder, proportionality with the square of the local water velocity is assumed.
The general concept of this hypothesis is confirmed by the model experiments. In the next chapter this will be discussed in more detail.

2 Equations of Motion

2.1 Introduction

If we are forming a mathematical model and we start from the fact that the hydrodynamic forces are functions of the velocities and accelerations involved in a motion, we can expand these forces - as has been done by Abkowitz (1964) - in a Taylor series of these velocities and accelerations. On the ground of considerations of magnitude we can ignore the terms the order of which is higher than the third e.g. There are some objections to this procedure however. Considering a term proportional to the third power of the angular velocity e.g. then the omission of the fourth-order terms means that the contribution of this term, regardless the forward speed, remains proportional with the third power of the angular velocity. From model experiments it is known that this - and similar terms - are reversed proportional with

the forward speed. Neglecting this speed dependence consequently corresponds with underestimating the non-linear effects described by these third order terms in the case of speed reduction. For a speed reduction of 50 percent, such a non-linear effect is underestimated by a factor two.
Another objection, though of less importance, is that if considering the separate velocities as lateral, forward and angular velocity, the particular role played by the forward speed hardly comes forward.

In section 2.3, a different basis has been chosen for the mathematical model, using the hypothesis mentioned in chapter 1. It will be shown that the non-dimensional variables involved are related to well-known quantities, like drift angle, radius of curvature and their change with respect to the distance covered by the ship.
The effects of the fourth degree terms, mentioned above, is involved in the third degree Taylor expansion of the forces, if they are considered functions of these characteristic variables.
It is emphasised however, that the concept of this is not new, because also Davidson and Schiff (1946), Nomoto (1957) and Eda and Crane (1962) already paid attention to the importance of these variables. Both earlier work and the present investigation, justify the adoption of the hypothesis concerning the forces.

2.2 Components of Hydrodynamic Forces

The equations of motion describing the balance of forces and moments during a still water manoeuvre can be written as follows (see also Figure 1):

$$\begin{aligned} m \cdot \left(\dot{v} + U_x r \right) &= Y \\ I_{zz} \cdot \dot{r} &= N \\ m \cdot \left(\dot{U}_x - v r \right) &= X \end{aligned}$$

Equation 1-a,b,c

where Y represents the component of the hydrodynamic forces perpendicular to the ship and N the corresponding moment, while X represents the component of these forces acting in longitudinal direction.
The sum of the hydrodynamic forces can be divided into three groups. The first group contains the components, which depend on the condition of motion of the ship without propeller and rudder. The variables involved in this case will be discussed in section 2.3.
The second group contains the forces, which act on the rudder. They depend on the effective angle of attack of the rudder, and as this quantity depends on the ship's condition of motion, these components will depend on the variables of the first group as well as on the rudder angle itself.
The third group contains the force components, which are - among others - caused by the change of circulation around the ship, due to the rudder deflection. In general, these components are considered to be the result of the fact that the sum of the hydrodynamic forces is not obtained by the superposition of the forces acting on the hull and those on the rudder, which may be approximately true for the side forces on sailing yachts.
Concerning the longitudinal force balance, a fourth group has to be considered, which involves the forces due to the resistance and the change of thrust caused by speed loss during

manoeuvring. This group determines the difference between the forward speed of the centre of gravity and the speed of the water near the rudder.

2.3 Some Considerations Concerning the Similarity of Conditions of Motion

In general, the variables - which describe the condition of motion of a line-piece $\overline{AB}$ in a horizontal plane - are:

$$\dot{x}_0, \ddot{x}_0, \dddot{x}_0, \ldots\ldots$$
$$\dot{y}_0, \ddot{y}_0, \dddot{y}_0, \ldots\ldots$$
$$\dot{y}, \ddot{y}, \dddot{y}, \ldots\ldots$$

where $\dot{x}_0$ and $\dot{y}_0$ represent the displacements of the middle of the line-piece in the direction of the x_0- and y_0-axis respectively. Consequently these variables and their derivatives determine the path, while $\dot{y}$ determines the change of the angle between the line-piece and the x_0-axis.

The description of the motion of a line-piece with these variables fixes this motion in space as well as in time. In the first instance we can leave the time - and consequently the velocities with which the motions are executed - out of consideration and describe them as a function of an infinitesimal displacement in the direction of the path.

The motion of the line-piece $\overline{AB}$ is then given by the equations:

$$x_0 = x_0(s)$$
$$y_0 = y_0(s)$$
$$y = y(s)$$

which is illustrated in the next figure.

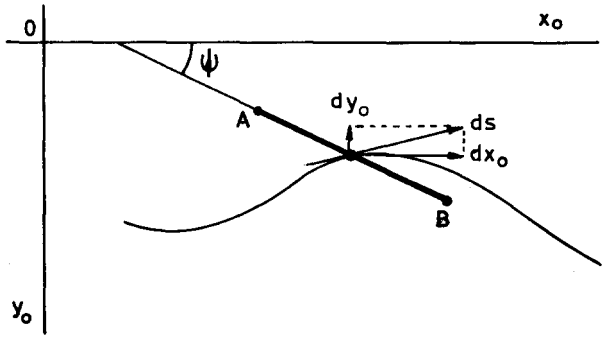

If we compare the motions of two line-pieces which have different lengths L_1 and L_2, we can call these motions *similar in space* if both the motions can be described by the following functions:

$$x_0^* = f_1(s^*)$$
$$y_0^* = f_2(s^*)$$
$$y = f_3(s^*)$$

where $x_0^* = x_0 / L$, $y_0^* = y_0 / L$ and $s^* = s / L$.

If these functions and their derivatives are continuous on a fixed interval of s^*, then for each value of these independent variables the following functions are also equal for both the motions:

$$\frac{\partial x_0^*}{\partial s^*}, \frac{\partial^2 x_0^*}{\partial s^{*2}}, \frac{\partial^3 x_0^*}{\partial s^{*3}}, \ldots\ldots$$
$$\frac{\partial y_0^*}{\partial s^*}, \frac{\partial^2 y_0^*}{\partial s^{*2}}, \frac{\partial^3 y_0^*}{\partial s^{*3}}, \ldots\ldots$$
$$\frac{\partial y}{\partial s^*}, \frac{\partial^2 y}{\partial s^{*2}}, \frac{\partial^3 y}{\partial s^{*3}}, \ldots\ldots$$

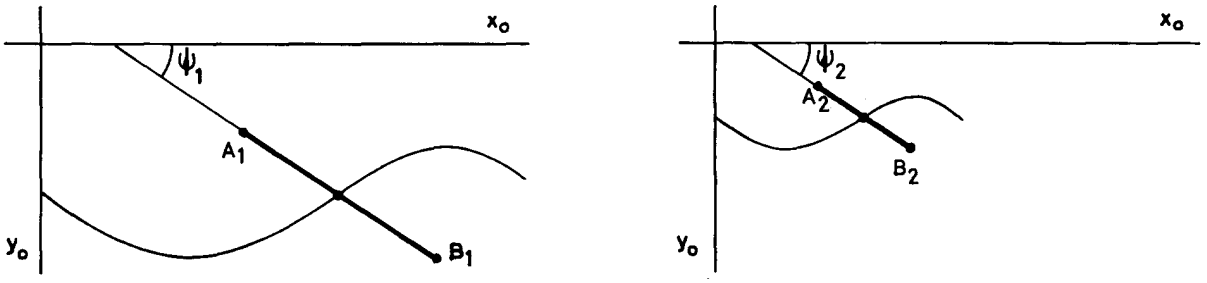

Therefore we can also state that the similarity of motions, starting from the same initial condition concerning the co-ordinate system, is determined by the above derivatives. On this ground we will further call them similarity parameters.

If we also involve the time t as the fourth dimension in the description of motions together with x_0, y_0 and y, we can speak of similarity in space as well as of similarity in space and time.
Just as the length-ratio of the line-pieces could have an arbitrary value, also the "time-ratio" can have any value.
Suppose the ratio of the times, necessary to cover the unit of displacement, has the value m, so that $\frac{\partial t_1}{\partial s^*} = m \cdot \frac{\partial t_2}{\partial s^*}$. If then T_1 and T_2 are constant (auxiliary) times, in such a way that their ratio has also the value m, then we define $t_1^* = \frac{t_1}{T_1}$ and $t_2^* = \frac{t_2}{T_2}$. For both the motions now $\frac{\partial t^*}{\partial s^*}$ has the same value. The motions of both the line pieces are now defined similar in space and time if on a certain interval of s^*, next to the functions f_1, f_2 and f_3, also for both the motions the function

$$t^* = f_4(s^*)$$

has the same value. Assuming this function and its derivatives are continuous, this also implies the equality of the following functions

$$\frac{\partial t^*}{\partial s^*}, \frac{\partial^2 t^*}{\partial s^{*2}}, \frac{\partial^3 t^*}{\partial s^{*3}}, \ldots\ldots$$

As it is more convenient to consider speed-ratios than "time-ratios" we keep in mind that the speed U has been defined to be $\frac{\partial s}{\partial t}$. Consequently from the equality of $\frac{\partial t^*}{\partial s^*}$ it follows that

the two speeds have a constant ratio: $\frac{U_1}{U_2} = \frac{a}{m} = l$, where a are the length-ratio and m the time-ratio. In the next figure the meaning of the space and time similarity conditions have been sketched.

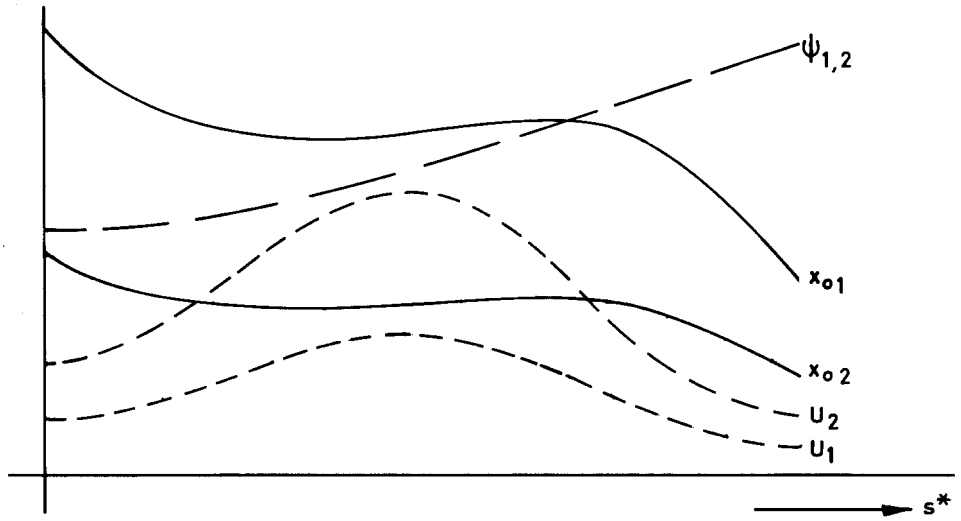

Similarity of motions in space and time provides:

$$\frac{y_{0_1}}{y_{0_2}} = \frac{x_{0_1}}{x_{0_2}} = a = \frac{L_1}{L_2}; \qquad \frac{y_1}{y_2} = 1; \qquad \frac{U_1}{U_2} = \frac{a}{m}; \qquad m = \frac{L_1/U_1}{L_2/U_2}$$

Anticipating the next chapter, we can imagine the two line pieces to be two submerged hydrofoils, which run along two similar paths. If in that case both the Reynolds numbers would be sufficiently high and the angles of attack sufficiently small then, regardless the ratio of the Reynolds numbers. Regardless the value of the product $a \cdot l$, this means that it might be expected that at each corresponding moment the hydrodynamic forces would be in the proportion of $\frac{1}{2} r U_1^{\,2} L_1^{\,2}$ to $\frac{1}{2} r U_2^{\,2} L_2^{\,2}$. Provided this would be exactly true, then we put the question what amount of instantaneous similarity of both the motions is necessary and sufficient so as to satisfy both the hydrodynamic forces the same proportion.

The fact is that if we could answer this question, we are also able to form a set of equations of motion for the hydrofoil, moving in the horizontal plane, for an equation of motion describes the equilibrium of forces instantaneously. In the first place we will illustrate that if we compare two different conditions of motion instantaneously, there is a question of the *amount of similarity.*

Considering the two motions sketched above, for which at each corresponding moment the variables $\frac{\partial x^*}{\partial s^*}$, $\frac{\partial y^*}{\partial s^*}$, $\frac{\partial y}{\partial s^*}$ and $\frac{\partial t^*}{\partial s^*}$ and all their derivatives have the same value, it will be clear that here is the question of the highest-order similarity. If we consider two motions and comparing them at a corresponding moment, assuming only a restricted number of derivatives of x^* , y^* , y and t^* to be equal at that moment, than we can state these motions to have a restricted similarity. This will be illustrated with an example.

Provided that at the moment considered only the following derivatives are equal for both the motions:

$$\frac{\partial x_0^{\,*}}{\partial s^*},\ \frac{\partial y_0^{\,*}}{\partial s^*},\ \frac{\partial y}{\partial s^*},\ \frac{\partial t^*}{\partial s^*},\ \frac{\partial^2 x_0^{\,*}}{\partial s^{*2}},\ \frac{\partial^2 y_0^{\,*}}{\partial s^{*2}},\ \frac{\partial^2 y}{\partial s^{*2}} \text{ and } \frac{\partial^2 t^*}{\partial s^{*2}}.$$

We then state there is a second-order similarity. Characterising a corresponding moment by the equality of y, which means a specified choice of the co-ordinate system, and using the following equalities:

$$\frac{\partial x_0^{\,*}}{\partial s^*} = \cos f \qquad \frac{\partial^2 x_0^{\,*}}{\partial s^{*2}} = -\sin f \cdot \frac{\partial f}{\partial s^*}$$

$$\frac{\partial y_0^{\,*}}{\partial s^*} = \sin f \qquad \frac{\partial^2 y_0^{\,*}}{\partial s^{*2}} = +\cos f \cdot \frac{\partial f}{\partial s^*}$$

then, at the corresponding moment, also are equal:

$$b_G = y - f \qquad \text{and} \qquad \frac{L}{R} = \frac{\partial f}{\partial s^*} \qquad \text{(see next figure)}$$

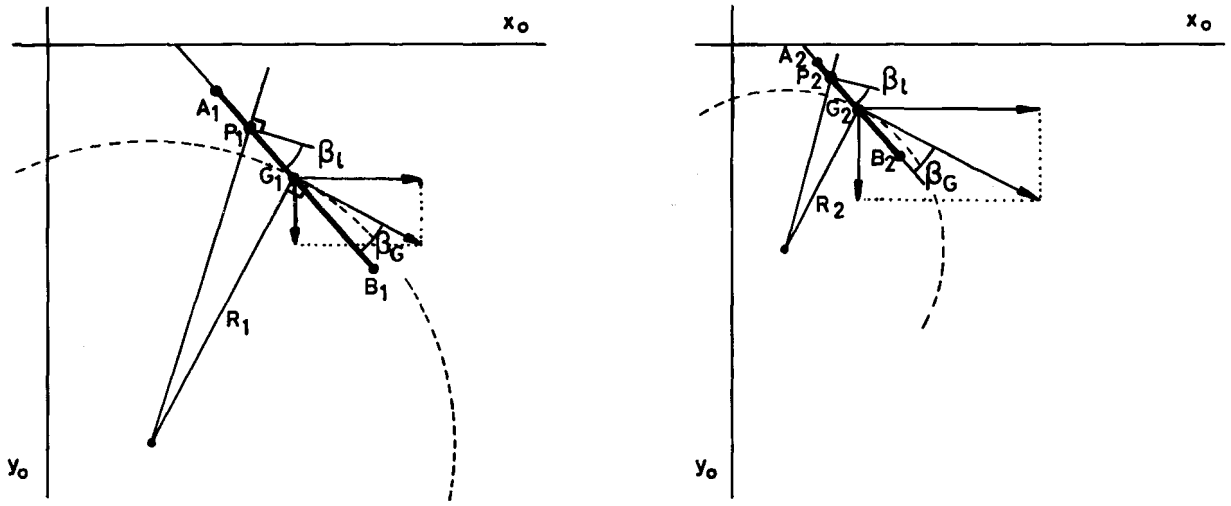

If we now consider the local "angle of attack" in P at distance x before G then is find:

$$b_1 \approx b_G - \frac{x}{L} \cdot \frac{\partial f}{\partial s^*}$$

Consequently this angle is equal for both the motions. The change of this angle appears not to be equal however, as follows from the fact that

$$\frac{\partial b_1}{\partial s^*} = \frac{\partial b_G}{\partial s^*} - \frac{x}{L} \cdot \frac{\partial^2 f}{\partial s^{*2}}$$

where $\frac{\partial^2 f}{\partial s^{*2}}$ is a function of $\frac{\partial^3 x_0^{\,*}}{\partial s^{*3}}$, which was not equal in both cases.
So we can speak of *restricted-similar instantaneous conditions of motion* indeed.

The principle of the restricted-similar conditions of motion is used to form the equations of motion of a body moving in a horizontal plane, particularly that of the manoeuvring ship.

This has to be done in such a way that the drawbacks attending the equations of motion, which describe the hydrodynamic forces being functions of the lateral velocity and acceleration and the angular velocity and acceleration non-dimensionalised with the initial speed or otherwise, are avoided.

2.4 Hypothesis Concerning Hydrodynamic Forces Acting on a Manoeuvring Ship

As has been discussed in the preceding chapter the hydrodynamic forces on two similar submerged bodies will be proportional to their force-units $\frac{1}{2} r U_1^2 L_1^2$ and $\frac{1}{2} r U_2^2 L_2^2$ at a certain moment, if their conditions of motion satisfy certain demands of similarity at that moment.

If these motions are rectilinear, this similarity is implied in the same value of the angle of attack and if the motions are non-stationary the principle of the restricted similarity of a certain order can be applied to the motions to be compared.

As a hypothesis concerning the hydrodynamic forces acting on two similar ships, we now state that - within a restricted range of length and speed (or time) ratios a and l (or m) - these forces will be proportional to the force units $\frac{1}{2} r U_1^2 L_1^2$ and $\frac{1}{2} r U_2^2 L_2^2$ at a certain moment, if - at the moment considered - both the conditions of motion satisfy specified similarity demands. These will have to be determined further.
We will now try to form the equations of motion for the manoeuvring ship in such a way that this hypothesis is expressed by it. In a first instance, we will only consider those forces that are independent of a rudder deflection and the instantaneous thrust, which means that only the first group forces (chapter 2.2), are described.
The general form of the hydrodynamic side force equation can then be expressed as follows:

$$Y = \frac{1}{2} r U^2 L^2 \cdot Y^*$$

where the equality of Y^*, if comparing two similar ships, has to express that the conditions of motion have a certain amount of similarity. This means that Y^* can only be a function of a number of similarity parameters, thus:

$$Y^* = Y^* \cdot \left(\frac{\partial^k x_0^*}{\partial s^{*k}}, \frac{\partial^k y_0^*}{\partial s^{*k}}, \frac{\partial^k y}{\partial s^{*k}}, \frac{\partial^k t^*}{\partial s^{*k}} \right) \qquad (k = 1, \ldots\ldots n)$$

where n has to be determined further.

The corresponding moment and longitudinal forces can be described in a similar way where it is noted that the latter contains an additional constant, expressing the longitudinal resistance to be proportional to the square of the forward speed in the considered range of speed and length ratios.

An essential point involved in this matter is that in general the hydrodynamic forces are assumed only functions of the velocities and accelerations involved which means that no higher derivatives of displacements and angles play a role. As there is a reversible relation between the velocities and accelerations at the one side and the similarity parameters on the other hand, this assumption contains a prescription of the amount of similarity.

It is not discussed here however to what extent this assumption is true. As can be seen simply, the amount of similarity concerned cannot be greater than of the second-order. For a third-order similarity e.g. the equality of $\frac{\partial^2 f}{\partial s^{*2}}$ is found, from which the equality of $\ddot{v}$ follows, the time derivative of the lateral acceleration.

Consequently for the further description of the hydrodynamic forces we assume that they are besides of the force unit $\frac{1}{2} rU^2L^2$, only functions of the parameters that determine the second-order similarity of instantaneous conditions of motions.

Thus:

$$\left.\begin{matrix} Y^* \\ N^* \\ X^* \end{matrix}\right\} = \left.\begin{matrix} Y^* \\ N^* \\ X^* \end{matrix}\right\} \left\{\begin{matrix} \frac{\partial x_0^*}{\partial s^*}, \frac{\partial y_0^*}{\partial s^*}, \frac{\partial y}{\partial s^*}, \frac{\partial t^*}{\partial s^*}, \\ \frac{\partial^2 x_0^*}{\partial s^{*2}}, \frac{\partial^2 y_0^*}{\partial s^{*2}}, \frac{\partial^2 y}{\partial s^{*2}}, \frac{\partial^2 t^*}{\partial s^{*2}}, \\ \text{Constants} \end{matrix}\right\}$$

In the appendix it is shown that from the equality of the second order similarity parameters follows the equality of the following variables:

$$\frac{v}{U}, \quad \frac{L \cdot r}{U}, \quad \frac{L \cdot \dot{v}}{U^2}, \quad \frac{L^2 \cdot \dot{r}}{U^2} \quad \text{and} \quad \frac{L \cdot \dot{U}}{U^2}$$

from which follows the connection between these similarity parameters and the velocities and accelerations.

The usefulness of this hypothesis, considering two identical ships, will depend on the speed ratio l. On the ground of Froude's law it might be expected that this value is sure to differ only little from unity. So, it has to be examined within what bounds this ratio can be changed, without disturbing the usefulness of the hypothesis. It also has to be examined to what extend the lengths ratio of the ships, if they are further similar, limits the use. So, it might be expected that the hypothesis can only be applied in a restricted range of length and speed ratios, in such a way that if wave generation can not be neglected. The Froude number should nearly have the same value, so as to be sure that the wave patterns of both ships would nearly be similar. This means that the ratio $l / \sqrt{a}$ should nearly be equal to unity in that case. If the comparison concerned two submerged bodies than the flow patterns would only be similar if the Reynolds number would be equal in both cases, which means that the product $a \cdot l$ would be equal to unity.

Summarising, it is to be expected that the usefulness of this hypothesis will depend on both Froude and Reynolds number. It is noted however, that if the hypothesis is applied to the longitudinal forces on surface ships, it is very likely that the limits of speed and lengths ratios will differ from those due to the lateral forces and moment. This is because it is already known that the longitudinal resistance is rather sensitive to scale effects, which means to l and a values.

If the hypothesis is also applied to the force components of the second group then the local similarity is characterised by the actual angle of attack of the rudder and its "path derivative". The actual angle of attack is assumed a linear function of the three angles involved, thus:

$$d_{eff} = p_1 \cdot d + p_2 \cdot v^* + p_3 \cdot r^*$$

which indicates that the variables characterising the similarity in this case are d , v^*, r^* and, if acceleration effects are considered, also the path-derivatives of these variables. This set of variables, completed with the local water velocity, determines the magnitudes of the force components of the second group.

Concerning the components of the third group, it is assumed that they will mainly depend on the variables of both the first and second group. They will partly be proportional to the square of the forward speed of the centre of gravity and for the rest to the square of the local (rudder) speed.

On this basis the mathematical model can be build up, considering the three groups to be functions of the non-dimensional variables, concerned. The expansion of the three groups in a third degree Taylor series leads to a number of terms a part of which being proportional with the square of the forward speed, while the remaining terms will be proportional to the square of the local rudder speed.
Considering e.g. the linear term in v^*, then the following expression is found:

$$\frac{1}{2}\cdot rL^2\cdot\left\{a_1 v^* U^2 \right. \qquad + a_2 v^* U_R{}^2 \qquad \left. + \left(a_{31}U^2 + a_{32}U_R{}^2\right)v^*\right\}$$

1st group (forces on hull without rudder and propeller)	2nd group (forces on rudder due to effective angle of attack)	3rd group (interaction rudder-hull; forces due to failing of superposition principle)

The expressions for the other terms will have similar forms. On this ground the mathematical model is to be written in the following form:

$$m\cdot\left(\dot{v}+U_x r\right)=\frac{1}{2}rU^2L^2Y_1^* + \frac{1}{2}rU_R{}^2L^2\overline{Y}_2$$

$$I_{zz}\cdot\dot{r}=\frac{1}{2}rU^2L^3N_1^* + \frac{1}{2}rU_R{}^2L^3\overline{N}_2$$

$$m\cdot\left(\dot{U}_x - vr\right)=\frac{1}{2}rU^2L^2X_1^* + \frac{1}{2}rU_R{}^2L^2\overline{X}_2 + X_3$$

Equation 2-a,b,c

In these equations the components marked with a star contain the terms originated from the Taylor expansions of the first and second group. The dashed components contain the corresponding terms of the second and third group. Both star and dash marked components are functions of the rudder angle and the five variables determine the second order similarity. The longitudinal force component X_3 describes the difference between the ship's straight-line resistance and the change of thrust due to the speed reduction.

On the ground of theoretical considerations and the experience from earlier investigations a number of assumptions have been made, which simplify the expressions for the various

components. Some of these assumptions have been investigated particularly, while others are not contradicted by the measurements.

The assumptions concerned are summarised as follows:

1. The forward speed U, as a variable of Equation 2, can be replaced by its longitudinal component U_x. Consequently, the variables v^* and r^* are defined as v/U_x and $L \cdot r/U_x$ respectively, while the unit ds^* is defined as $U_x \cdot dt/L$.
2. The hydrodynamic lateral forces are independent of the longitudinal acceleration, while the hydrodynamic longitudinal forces are independent of the sway and yaw accelerations.
3. Non-linear acceleration effects do not occur in the range of interest.
4. If the ship is on a straight course, the forces due to a certain rudder deflection are proportional to the square or the local rudder speed U_R. (This assumption may be considered the definition of the quantity U_R for the present investigations).
5. The influence of the rudder rate on added mass effects is negligible for practical purposes.

2.5 Set of Equations of Motion

Executing the Taylor expansions of the three groups of forces and moments and applying the assumptions indicated above, the equations of motion can be written as follows:

$$
\begin{aligned}
&\left\{m' - \left(Y_{\dot{v}}^* + \overline{Y}_{\dot{v}} \frac{U_R'^2}{(1+u')^2}\right)\right\}\dot{v}' - \left\{Y_{\dot{r}}^* + \overline{Y}_{\dot{r}} \frac{U_R'^2}{(1+u')^2}\right\}\dot{r}' = \\
&\left\{Y_v^*(1+u') + \overline{Y}_v \frac{U_R'^2}{1+u'}\right\}v' + \left\{(Y_r^* - m')(1+u') + \overline{Y}_r \frac{U_R'^2}{1+u'}\right\}r' + \\
&\left\{Y_{vvv}^* \frac{1}{1+u'} + \overline{Y}_{vvv} \frac{U_R'^2}{(1+u')^3}\right\}v'^3 + \left\{Y_{rrr}^* \frac{1}{1+u'} + \overline{Y}_{rrr} \frac{U_R'^2}{(1+u')^3}\right\}r'^3 + \\
&\left\{Y_{vrr}^* \frac{1}{1+u'} + \overline{Y}_{vrr} \frac{U_R'^2}{(1+u')^3}\right\}v'r'^2 + \left\{Y_{rvv}^* \frac{1}{1+u'} + \overline{Y}_{rvv} \frac{U_R'^2}{(1+u')^3}\right\}r'v'^2 + \\
&\left\{Y_{dvv}^* + \overline{Y}_{dvv} \frac{U_R'^2}{(1+u')^2}\right\}dv'^2 + \left\{Y_{drr}^* + \overline{Y}_{drr} \frac{U_R'^2}{(1+u')^2}\right\}dr'^2 + \\
&\left\{Y_{vdd}^*(1+u') + \overline{Y}_{vdd} \frac{U_R'^2}{1+u'}\right\}v'd^2 + \left\{Y_{rdd}^*(1+u') + \overline{Y}_{rdd} \frac{U_R'^2}{1+u'}\right\}r'd^2 + \\
&\left\{Y_{vrd}^* + \overline{Y}_{vrd} \frac{U_R'^2}{(1+u')^2}\right\}v'r'd + \left\{Y_a^*(1+u')^2 + \overline{Y}_a U_R'^2\right\} + \\
&\left\{\overline{Y}_d d + \overline{Y}_{dd} d^2 + \overline{Y}_{ddd} d^3\right\}U_R'^2
\end{aligned}
$$

Equation 3-a

$$\left\{I_{zz}' - \left(N_{\dot r}^{*} + \overline{N}_{\dot r}\frac{U_R'^2}{(1+u')^2}\right)\right\}\dot r' - \left\{N_{\dot v}^{*} + \overline{N}_{\dot v}\frac{U_R'^2}{(1+u')^2}\right\}\dot v' =$$
$$\left\{N_v^{*}(1+u') + \overline{N}_v\frac{U_R'^2}{1+u'}\right\}v' + \left\{N_r^{*}(1+u') + \overline{N}_r\frac{U_R'^2}{1+u'}\right\}r' +$$
$$\left\{N_{vvv}^{*}\frac{1}{1+u'} + \overline{N}_{vvv}\frac{U_R'^2}{(1+u')^3}\right\}v'^3 + \left\{N_{rrr}^{*}\frac{1}{1+u'} + \overline{N}_{rrr}\frac{U_R'^2}{(1+u')^3}\right\}r'^3 +$$
$$\left\{N_{vrr}^{*}\frac{1}{1+u'} + \overline{N}_{vrr}\frac{U_R'^2}{(1+u')^3}\right\}v'r'^2 + \left\{N_{rvv}^{*}\frac{1}{1+u'} + \overline{N}_{rvv}\frac{U_R'^2}{(1+u')^3}\right\}r'v'^2 +$$
$$\left\{N_{dvv}^{*} + \overline{N}_{dvv}\frac{U_R'^2}{(1+u')^2}\right\}dv'^2 + \left\{N_{drr}^{*} + \overline{N}_{drr}\frac{U_R'^2}{(1+u')^2}\right\}dr'^2 +$$
$$\left\{N_{vdd}^{*}(1+u') + \overline{N}_{vdd}\frac{U_R'^2}{1+u'}\right\}v'd^2 + \left\{N_{rdd}^{*}(1+u') + \overline{N}_{rdd}\frac{U_R'^2}{1+u'}\right\}r'd^2 +$$
$$\left\{N_{vrd}^{*} + \overline{N}_{vrd}\frac{U_R'^2}{(1+u')^2}\right\}v'r'd + \left\{N_a^{*}(1+u')^2 + \overline{N}_a U_R'^2\right\} +$$
$$\left\{\overline{N}_d d + \overline{N}_{dd}d^2 + \overline{N}_{ddd}d^3\right\}U_R'^2$$

Equation 3-b

$$\left\{m' - \left(X_{\dot u}^{*} + \overline{X}_{\dot u}\frac{U_R'^2}{(1+u')^2}\right)\right\}\dot u' =$$
$$\left\{X_{vv}^{*} + \overline{X}_{vv}\frac{U_R'^2}{(1+u')^2}\right\}v'^2 + \left\{X_{rr}^{*} + \overline{X}_{rr}\frac{U_R'^2}{(1+u')^2}\right\}r'^2 +$$
$$\left\{X_{vr}^{*} + m' + \overline{X}_{vr}\frac{U_R'^2}{(1+u')^2}\right\}v'r' + \left\{X_{rd}^{*}(1+u') + \overline{X}_{rd}\frac{U_R'^2}{1+u'}\right\}r'd +$$
$$\left\{X_{dv}^{*}(1+u') + \overline{X}_{dv}\frac{U_R'^2}{1+u'}\right\}dv' + \left\{\overline{X}_{dd}U_R'^2\right\}d^2 +$$
$$\left\{X_R^{*}(1+u')^2 - X_R^{*}\right\} + X_T'u'$$

Equation 3-c

In these equations all variables have been made non-dimensional with the initial speed U_0 so that e.g.:

$$u' = \frac{U_x}{U_0} - 1, \qquad v' = v^{*}(1+u') \quad \text{and} \quad r' = r^{*}(1+u')$$

Some additional remarks concerning these equations:

a. The side force and moment equations contain some terms to describe the asymmetrical behaviour of the ship. With zero rudder deflection these terms are $Y_a^{*}(1+u')^2 + \overline{Y}_a U_R'^2$

and $N_a^*\left(1+u'\right)^2 + \overline{N}_a U_R'^2$ while the asymmetrical rudder effectiveness is described by the terms $\overline{Y}_{dd} d^2$ and $\overline{N}_{dd} d^2$ respectively.

b. The longitudinal force component X_3 is divided into two components, the first of that describes the balance between the original thrust and the straight-line resistance while the second describes the (linearised) increment of the thrust during a manoeuvre.

c. The fourth degree terms, which were mentioned in the introduction, are due to the factors $1/\left(1+u'\right)$, which may be linearised in the range $-0.60 < u' < 0.00$ to $0.84 - 2.30 \cdot u'$.

d. If the change of speed during a manoeuvre is larger than the range in which the hypothesis is valid, than the star and dash coefficients can be considered linear functions of the speed. In that case additional coefficients as Y_{vu}^* and $\overline{Y}_{vu}$ should be added. For the present investigation, this appeared not necessary however.

3 Execution of Tests

3.1 Measuring Equipment

The principal property of the measuring equipment is that only harmonic components of the forces are determined. For the present investigation only the first harmonic components were needed. This determination is achieved by multiplying the forces by $\sin wt$ and $\cos wt$ respectively, while these products are integrated during one or more periods of the oscillation. The non-oscillatory components of the forces are determined by integration of the force during a number of periods. Zunderdorp and Buitenhek (1963) give in a more detailed discussion on the oscillator and the measuring equipment.
The static drift angle adjustment during the oscillation tests is achieved by turning the model with respect to the connecting line of the oscillator struts (the “pure yawing line”). This is sketched in Figure 2.

3.2 Determination of Draught and Trim

As the model was restrained from heaving and pitching the draught and trim, as dependent on the forward speed and the number of propeller revolutions had to be determined.
The revolutions adjusted for these tests were estimated from the available full-scale data. A change of the rpm did influence neither the mean draught nor the trim however. In the next table the various draughts fore and aft are given for model and ship.

MODEL			SHIP		
U_0 (m/sec)	Draught fore (mm)	Draught aft (mm)	U_0 (kn)	Draught fore (ft)	Draught aft (ft)
1.080	236.0	229.3	15.5	42.6	41.4
0.864	232.7	229.1	12.4	42.0	41.3
0.648	230.3	229.0	9.3	41.5	41.3
0.432	228.9	228.3	6.2	41.3	41.2
0.000	227.2	227.2	0.0	41.0	41.0

Table 1 Draught and Trim

These draughts have been adjusted for the tests concerned. It is questioned however if it is correct to restrain the model in vertical direction during oscillation and other tests. A particular investigation might give the answer, but it is not expected that undesirable cross-coupling effects would disturb the side force measurements, due to the uncoupling of the swaying and yawing motion. This is also expected with respect to the rolling motion. As it was not the purpose of this investigation to find an answer to this question, it was considered a useful approximation to adjust the constant draughts, derived from straight-line tests and to restrain the model also from rolling.

3.3 Determination of Resistance and Propulsion Coefficients

The description of the balance between longitudinal resistance and the propeller thrust is partly based on some full-scale measurements of rpm at 15.5 knots and partly on the propeller characteristics. From these data the wake fraction was derived while for the lower speeds, caused by manoeuvring, this wake fraction was considered constant. From the fact that during a manoeuvre the power does not change, the increment of thrust and the decrement of rpm could be calculated using the propeller characteristics. For comparison purposes also the full-scale measurements of these quantities are given in Figure 3 and Figure 4. Concerning the other initial speeds, 12.4, 9.3 and 6.2 knots, a linear relation between these speeds and the rpm was adopted (see Figure 5). The increment of thrust and the decrement of the rpm during manoeuvres with these initial speeds were determined as this was done for the 15.5 knots initial speed.
In Figure 6 and Figure 7 the calculated thrust and torque are plotted for the initial conditions.
It can be shown that on a straight course a parabolic relation between the thrust and the forward speed exists, provided the thrust curve of the propeller diagram is linearised in the range of interest. Consequently the assumption of a parabolic relation between the longitudinal resistance and the speed is equivalent to the assumption of a speed-independent thrust deduction fraction. This number was estimated to be 0.20. On this basis the resistance coefficient X_R^* was calculated:

$$X_R^* = -54.0 \cdot 10^{-5}$$

while for the effective thrust increment coefficient X_T' was found:

$$X_T' = -25.0 \cdot 10^{-5}$$

In Table 2 the computed rps, concerning the various conditions, are summarised. It is noted however that these data are corrected for the differences between the full-scale and model propeller (U 218 - B 5.60 respectively).

U_0 = 1.080 m/s			U_0 = 0.864 m/s			U_0 = 0.648 m/s			U_0 = 0.432 m/s		
U_x	u'	rps	U_x	u'	rps	U_x	u'	rps	U_x	u'	rps
1.080	0.00	12.85									
0.864	-0.20	12.30	0.864	0.00	10.23						
0.648	-0.40	11.80	0.648	-0.25	9.70	0.648	0.00	7.73			
0.432	-0.60	11.32	0.432	-0.50	9.21	0.432	-0.33	7.20	0.432	0.00	5.12

Table 2 Model Speed and Propeller Rate

The rps values, adjusted during the model tests, are not the same as given in this table however, as originally these values were based on the full-scale relation between thrust and speed as given by Clarke (1965). During the analysis of the test data this relation did not appear to correspond with the full-scale data of rpm and the propeller diagram, consequently nor did the rpm-U relation. This is shown in Figure 8. From this figure it is assumed that the full-scale speed measurements concerned are not correct. As, in addition, the coefficients, which describe the balance between resistance and thrust during a manoeuvre based on this relation, resulted in very large differences between the computed manoeuvres and those executed on full-scale, the linear relation between rpm and speed was adopted. The coefficients of the force and moment components $\overline{Y}_2$, $\overline{N}_2$ and $\overline{X}_2$ have been corrected as far as necessary, which was possible because their relation with the rpm was known from the model experiments.

3.4 Determination of Rudder Speed U_R

The quantity U_R has been derived from the straight-line tests with constant rudder angle. These tests were executed for the 10 combinations of speed and rps, while in each case the rudder angle was varied from 36 degrees port to 36 degrees starboard with steps of 9 degrees. A formal description of the water velocity near the rudder has been based on the impulse theory with respect to the propeller. According to this theory the water velocity at a certain distance from the propeller disk can be written as:

$$U_R' = V_e' + m \cdot C_a'$$

Equation 4

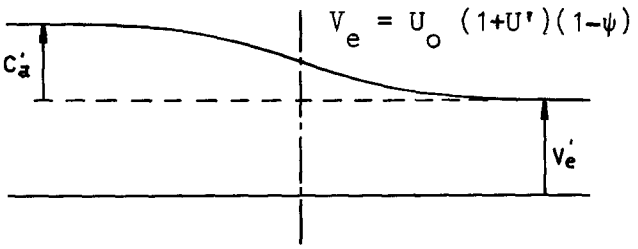

where the prime denotes making it non-dimensional with the initial speed U_0. If the curves of the propeller torque and thrust are linearised in the speed range of interest the expression for C_a' can be written as follows:

$$\left(\frac{C_a'}{V_e'} + 1\right)^2 = 1 + \frac{a_2}{\Lambda} + \frac{a_1}{\Lambda^2}$$

Equation 5

where the coefficients a_1 and a_2 describe the linearised torque and thrust.

Using the thrust deduction fraction y, as derived in Chapter 3.3, the values of C_a' can be calculated for each of the 10 speed-rps combinations given in Table 2. If these values are applied to Equation 5, the unknown speed U_R' is replaced by the quantity m, which originally indicated the distance from the propeller disk. It must be noted however that in this case the deviations due to the assumptions used culminate at the computation of m, so that

this quantity rather has to be considered a calculation-quantity than an indication for the distance between rudder and propeller. The same is to be applied to the quantity U_R'.
Substitution of the expression for U_R' into the formal description of the side force and moment measurements at $v^* = r^* = 0$, for each of the rudder angles applied, a value of m was obtained. In the next figure the products $m \cdot d$ has been plotted versus the rudder angle from which the optimal value of 0.376 was derived.

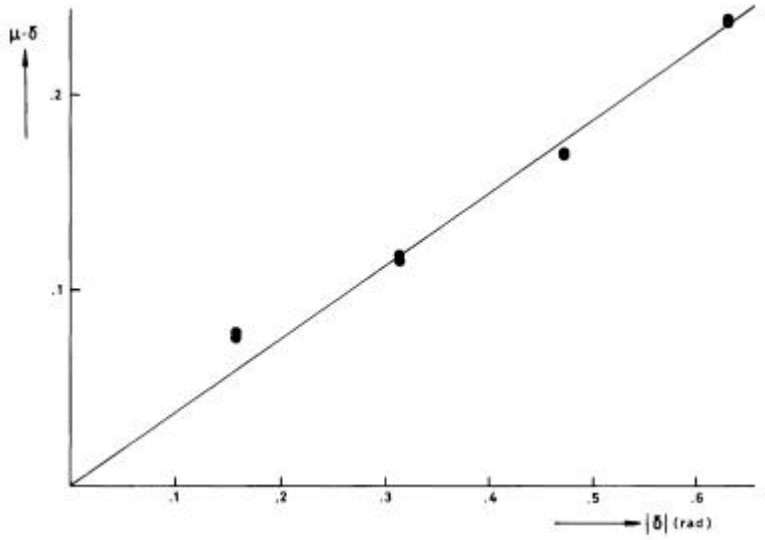

Using this value of m, the values of $U_R'^2$ were calculated and plotted in Figure 36-c versus the relative speed loss u'.

In Figure 9, for the 10 combinations of speed and rpm the measured rudder forces and moments are plotted on the basis of $U_R'^2$ while the rudder angle is a parameter.
The values of Y_a and N_a were too small to distinguish between star and dash components. A mean value, derived from the swaying tests and the present tests is obtained. For the computation of the rudder coefficients, the measurements concerned were corrected with these mean values.

3.5 Determination of Remaining Coefficients

3.5.1 Static Sway Tests

These tests, executed at the 10 combinations of speed and rpm, provided the coefficients of the following variables:

Y and N equation: v^*, v^{*3}, $v^* d^2$, $v^{*2} d$

X equation: v^{*2}, $v^* d$

while also the Y_a and N_a coefficients were determined.

In Table 3 a scheme of the test program concerned is given.

Actual Speed		1.08 m/sec	.86 m/sec		.65 m/sec			.43 m/sec		
R.p.s.		12.38	11.95	10.29	11.54	9.85	8.34	11.20	9.53	8.00	6.50
β	$\lvert v^* \rvert$										
$\pm 4^\circ$	.0698	θ	θ	θ	θ	θ	θ	θ	θ	θ	θ
$\pm 8^\circ$	.1392	θ	θ	θ	θ	θ	θ	θ	θ	θ	θ
$\pm 12^\circ$	.2079	θ	θ	θ	θ	θ	θ	θ	θ	θ	θ
$\pm 13.8^\circ$	.2385		θ	θ	θ	θ	θ	θ	θ	θ	θ

Combined drift and rudder tests	$\lvert\delta\rvert$	9	18	27	36	9	18	27	36	9	18	27	36	9	18	27	36	9	18	27	36	9	18	27	36
	+	θ	θ	θ	θθ	θ	θ	θ	θθ	θ	θ	θ	θθ	θ	θ	θ	θθ	θ	θ	θ	θθ	θ	θ	θ	θ
	−	θ	θ	θ	θθ	θ	θ	θ	θθ	θ	θ	θ	θθ					θ	θ	θ	θθ				
β = 0	+	θ	θ	θ	θθ	θ	θ	θ	θθ	θ	θ	θ	θθ	θ	θ	θ	θθ	θ	θ	θ	θθ	θ	θ	θ	θ
	−	θ	θ	θ	θθ	θ	θ	θ	θθ	θ	θ	θ	θθ	θ	θ	θ	θθ	θ	θ	θ	θθ	θ	θ	θ	θ

θ indicates that test has been executed

$v^* = -\sin\beta$

Table 3 Experimental Program of Static Sway Tests

Using the test results at $d = 0$ the coefficients of v^*, v^{*3} and v^{*2} are determined while computing the $v^* d^2$, dv^{*2} and $v^* d$ coefficients; the coefficients first mentioned were considered to be known quantities.

In Figure 10, Figure 11 and Figure 12, the side force and moment measurements concerned are plotted, while the longitudinal force measurements are shown in Figure 20, Figure 21 and Figure 23.

As no information was available involving the influence of the rudder speed U_R, the dash coefficients concerned could not be determined.

3.5.2 Oscillatory Swaying Tests

These tests were mainly executed to determine the lateral added mass effect. Only two initial speed conditions are considered while the influence of a change of rpm appeared negligible. Consequently $\overline{Y}_{\dot{v}}$ and $\overline{N}_{\dot{v}}$ are set to zero. The range in which the non-dimensional acceleration $L \cdot \dot{v} / U_x^2$ was changed; it was extended to 0.25 though an estimation of the maximum full-scale value is about 0.15. Nevertheless the measured force appeared linear with the acceleration in the whole range.
In Figure 13 the data concerned are plotted where the speeds are considered parameter.

3.5.3 Oscillatory Yawing Tests with Constant Drift and Rudder Angle

In general these tests were also executed for the 10 conditions given in Table 2. The amplitude of the characteristic variable r^* was varied between 0.05 and 0.70 corresponding with turning radii of approximately 20 and 3 ship lengths respectively.

The choice of the oscillator frequency has been based on the following considerations:

a. Based on the tank width available and the properties of the oscillator, the non-dimensional frequency $g = w \cdot U_x / g$ - which is the leading factor determining the oscillatory part of the wave pattern - was kept as small as possible. Concerning the influence of this variable the reader is referred to Van Leeuwen (1964).
b. The forces involved in the lowest speed, corresponding with a Froude number 0.07, had to be reasonably measurable.

In order to judge the frequency range used at these oscillatory motions, the quantity $2p / w^*$ can be used, indicating the number of ship lengths sailed during one period.
The restricted tank width and oscillator amplitude involve a disagreement between the forced motions of the model and full-scale manoeuvres e.g. sinus-response tests. These full-scale manoeuvres involve rather large amplitudes in the range of practical full-scale frequencies. It is not known however how far this discrepancy between model-scale and full-scale manoeuvres influences the hydrodynamic derivatives. In references Van Leeuwen (1969a) and Van Leeuwen (1969b) some more details concerning this matter are discussed.

In Table 4, a scheme of the complete yawing program is given.

Table 4 Experimental Program of Yaw Tests

Actual Speed		1.08 m/sec	.86 m/sec		.65 m/sec			.43 m/sec			
R.p.s.		12.38	11.95	10.29	11.54	9.85	8.34	11.20	9.53	8.00	6.50
r_o^*	$2\pi/\omega^*$	γ									
.05	5.03	.037									
.10	3.53	.053									
.15	2.87	.065			.019	.019	.019				
.20	2.47	.075	.048	.048	.027	.027	.027	.012	.012	.012	.012
.25	2.20							.013	.013	.013	.013
.30	1.99		.060	.060	.033	.033	.033	.015	.015	.015	.015
.35	1.83							.016	.016	.016	.016
.40	1.70		.070	.070	.039	.039	.039	.017	.017	.017	.017
.50	1.51		.079	.079	.044	.044	.044				
.60	1.36		.087	.087	.049	.049	.049 [1]				
.70	1.24		.096	.096	.054	.054	.054 [1]				
driftangle (degr)		0 4 8 12	0 4 8 12	0 4 8 12	0 4 8 12	0 4 8 12	0 4 8 12	0 4 8 12	0 4 8 12	0 4 8 12	0 4 8 12
rudder-angle (degr.)	0	θ θ θ θ	θ	θ θ θ θ	θ	θ	θ θ θ θ	θ	θ	θ	θ
	12	θ	θ	θ	θ	θ	θ	θ	θ	θ	θ
	18										
	24	θ	θ	θ	θ	θ	θ	θ	θ	θ	θ
	36	θ	θ	θ θ θ θ	θ	θ	θ θ θ θ	θ	θ	θ	θ

θ indicates that test has been executed

1) test only executed at $\delta = \beta = o$

$r^* = \frac{L}{U_x}.r \qquad \omega^* = \frac{L}{U_x}.\omega \qquad \gamma = \frac{\omega.U_x}{g}$

$2\pi/\omega^*$ = number of shiplengths sailed during one period of oscillation.

The measured forces and moments concerning these tests are to be divided into three components:
a. proportional to the angular velocity (sine component)
b. proportional to the angular acceleration (cosine component)
c. the constant component.

In Table 5, the various components are summarised while the variables concerned are mentioned in the sequence of determination.

sin θ component		cosine comp.	constant component		variables
Y, N	X	Y, N	Y, N	X	varied
r^*, r^{*3} $r^* v^{*2}$ $r^* \delta^2$ $r^* v^* \delta$	$r^* v^*$ $r^* \delta$	$L^2 \dot{r}/U_x^2$	$v^* r^{*2}$ δr^{*2}	r^{*2}	r^* r^*, v^* r^*, δ r^*, v^*, δ

Table 5 Variables and Components

Due to the criteria given in the preceding chapter, concerning the ranges of oscillator frequencies and amplitudes, the maximum value of the angular acceleration amplitude exceeds the corresponding value ever occurring at the full-scale ship, the latter being estimated about 1.30.
Consequently the coefficients concerned have been determined in this full-scale range the more so as outside this range the model experiments showed a considerable non-linear effect.
In Figure 14 through Figure 19 the side force and moment measurements are plotted, while in Figure 22, Figure 24 and Figure 25 the corresponding longitudinal force measurements are given.

3.6 Some Experiments with a Small Model (a = 100)

For comparison purposes, the results of a restricted number of tests with a small model are given. These tests had been executed before those with the larger model. Because of the very low speeds involved the results are considered not very trustworthy.
The test program consisted of:
a. static sway tests
b. oscillatory swaying tests
c. oscillatory yawing tests (without rudder angle and drift angle)

The influence of the speed reduction and consequently of the thrust increment was not examined in particular. It was assumed that the hypothesis mentioned in chapter 2.4 would hold. This means that the tests only had to be executed for the initial speed conditions.

In Table 6 the results of these tests are summarised and are compared with those of the large model. In Figure 26 through Figure 35 the measurements are shown.

Coefficients of small model (1:100)								
important coefficients					less important coefficients			
coeff.	1:55 model	1:100 model	diff. °/o		coeff.	1:55 model	1:100 model	diff. °/o
Y'_v	-1797	-1634	9		Y'_{vvv}	-8867	-11977	35
$Y'_r - m'$	- 774	- 863	12		Y'_{rrr}	+ 404	+ 303	25
Y'_δ	+ 330	+ 294	11		$Y'_{\delta\delta\delta}$	- 47	- 40	16
N'_v	- 473	- 473	0		N'_{vvv}	- 620	+ 360	150
N'_r	- 252	- 200	21		N'_{rrr}	- 270	- 323	20
N'_δ	- 164	- 132	19		$N'_{\delta\delta\delta}$	+ 27	+ 23	16
$m' - Y'_{\dot{v}}$	+2277	+2303	1		$N'_{\dot{v}}$	- 40	- 27	33
$I'_{zz} - N'_{\dot{r}}$	+ 128	+ 117	8		$Y'_{\dot{r}}$	- 65	- 28	57

Table 6 Coefficients of Small Model

As follows from Table 6 for the important coefficients the magnitude of the differences between the coefficients of the large and the small model is about 10 percent while this percentage for the less important coefficients is about 25. The importance of these differences is partly shown in Table 7 in which the results of a turning circle manoeuvre are given computed with the 1:100 model coefficients, completed with some of the large model.

$\delta o = -19^\circ$			
scale	1:100	1:55	full scale
advance (m)	993	985	972
transfer (m)	665	687	660
tactical diam. (m)	1255	1276	1233
diameter (m)	1086	1071	1100
r (degr./sec.)	.453	.466	.490
U^c (kn.)	8.48	8.59	9.10
β^x(degr.)	10.5	9.9	9.5

Table 7 Turning Circle Characteristics

Concerning the range of variables applied with this model it is noted that nearly the same maximum values of rudder angle, drift angle and angular velocity were adjusted. The difference between the frequency ranges of the two models is expressed by the two quantities

$2p/w^*$, denoting the number of ship lengths covered during one period of the oscillation, and g which quantity governs the wave pattern during the oscillatory motion.

The first quantity varies from 3.0 at $r_0^* = 0.10$ to 1.1 at $r_0^* = 0.50$, which is nearly the same range as is applied for the large model. The maximum value of g at $r_0^* = 0.50$ (0.17) is about two times the corresponding value of the large model however. Nevertheless, this value is considered sufficiently low as to avoid disturbing influences of this parameter.
Putting the results of the two models in the light of the hypothesis mentioned in chapter 2.4, it appears that the hypothesis holds for both models separately, but not if comparing both models. As in both cases the Froude numbers had the same values, the differences between the corresponding coefficients can be traced to the small Reynolds number of the small model.

3.7 Some Remarks Concerning Computed Coefficients

It is found that the rpm effect on the linear terms is very small, compared to the magnitude of these terms. Concerning the non-linear terms, it was not possible to distinguish between the normal scatter of the data and this rpm effect, due to the restricted accuracy of the measurements and the relatively small values of this non-linear term. This does not apply to the pure rudder-angle-dependant terms of course, the change of which with rpm is considerable.

Another important result is the usefulness of the hypothesis, concerning the proportionality of the forces with the square of the instantaneous speed and the characteristic variables v^* and r^*. This is clearly shown e.g. in Figure 10, Figure 11 and Figure 14. Though it has also been tried to distinguish between the results concerning the four initial speeds by Van Leeuwen (1969c), it follows from the figures just mentioned that the differences, which could be considered a Froude number effect are not significant however.

In Table 8, Table 9 and Table 10 in the left columns the coefficients of the set of Equation 3 are given while in the right columns the corresponding coefficients of Equation 4 are summarised, the latter being derived from the preceding ones. This derivation is partly based on the following approximations:

$$(1+u')^2 = 0.940 + 1.400 \cdot u'$$

$$\frac{1}{1+u'} = 0.837 - 2.300 \cdot u'$$

$$U_R'^2 = 0.709 + 0.632 \cdot u'$$

The accuracy of these approximations is shown in Figure 36 in which these quantities are plotted. Concerning the signs of the coefficients in these tables the rule holds that all terms are transported to the right hand sides of the equations.

LATERAL FORCE COEFFICIENTS ($*10^5$)						
"Star"-model eq.(3a)			"Prime"-model eq.(4a)			
$var.^*$	$C^*_{var.}$	$\overline{C}_{var.}$	$var.'$	$C'_{var.}$	$var'u'$	$C'_{var.u}$
v^*	-1797	0	v'	-1797	$v'u'$	-1797
r^* 1)	- 774	0	r' 1)	- 774	$r'u'$	- 774
δ	0	+330	δ	+ 234	$\delta u'$	+ 208
v^{*3}	-8867	0	v'^3	-7423	v'^3u'	+20394
r^{*3}	+ 404	0	r'^3	+ 339	r'^3u'	- 930
δ^3	0	- 47	δ^3	- 34	δ^3u'	- 30
v^*r^{*2}	-2208	0	$v'r'^2$	-1848	$v'r'^2u'$	+5078
$v^*\delta^2$	+ 277	0	$v'\delta^2$	+ 277	$v'\delta^2u'$	+ 277
r^*v^{*2}	+2562	0	$r'v'^2$	+2145	$r'v'^2u'$	-5893
$r^*\delta^2$	0	0	$r'\delta^2$	0	$r'\delta^2u'$	0
δv^{*2}	+ 652	0	$\delta v'^2$	+ 652	$\delta v'^2u'$	0
δr^{*2}	+ 218	0	$\delta r'^2$	+ 218	$\delta r'^2u'$	0
$v^*r^*\delta$	+ 412	0	$v'r'\delta$	+ 412	$v'r'u'$	0
δ^2	0	+ 40	δ^2	+ 28	δ^2u'	+ 25
1	- 14	0	1	- 13	u'	- 20
$L\dot{v}/U^2_x$ 1)	-2278	0	$\dot{v}'$ 1)	-2278	$\dot{v}'u'$	0
$L^2\dot{r}/U^2_x$	- 65	0	$\dot{r}'$	- 65	$\dot{r}'u'$	0

1) These coefficients include the ship's mass m'.

Table 8 Lateral Force Coefficients

MOMENT COEFFICIENTS ($\times 10^5$)						
"Star"-model eq.(2b)			"Prime"-model eq.(3b)			
var.*	$C^*_{var.}$	$\overline{C}_{var.}$	var.'	$C'_{var.}$	var.'u'	$C'_{var.u}$
v^*	- 473	0	v'	- 473	$v'u'$	- 473
r^*	- 252	0	r'	- 252	$r'u'$	- 252
δ	0	- 164	δ	- 116	$\delta\, u'$	- 103
v^{*3}	- 620	0	v'^3	- 519	v'^3u'	+1425
r^{*3}	- 270	0	r'^3	- 226	r'^3u'	+ 620
δ^3	0	+ 27	δ^3	+ 19	δ^3u'	+ 17
v^*r^{*2}	+ 395	0	$v'r'^2$	+ 331	$v'r'^2u'$	- 908
$v^*\delta^2$	- 69	0	$v'\delta^2$	- 69	$v'\delta^2u'$	- 69
r^*v^{*2}	-2191	0	$r'v'^2$	-1834	$r'v'^2u'$	+5040
$r^*\delta^2$	0	0	$r'\delta^2$	0	$r'\delta^2u'$	0
δv^{*2}	- 235	0	$\delta v'^2$	- 235	$\delta'v'^2u'$	0
δr^{*2}	- 104	0	$\delta r'^2$	- 104	$\delta r'^2u'$	0
$v^*r^*\delta$	- 232	0	$v'r'\delta$	- 232	$v'r'\delta u'$	0
δ^2	0	- 12	δ^2	- 8	δ^2u'	- 7
1	0	0	1	0	u'	0
$L\dot{v}/U_x^2$	- 40	0	$\dot{v}'$	- 40	$\dot{v}'u'$	0
$L^2\dot{r}/U_x^2$ [1)]	- 128	0	$\dot{r}'$ [1)]	- 128	$\dot{r}'u'$	0

[1)] These coefficients include ship's moment of inertia I'_{zz}

Table 9 Yaw Moment Coefficients

LONGITUDINAL FORCE COEFFICIENTS ($\times 10^5$)						
"STAR"-MODEL (eq.2c)			"PRIME"-MODEL (eq.3c)			
var^*	C^*_{var}	$\overline{C}_{var}$	var'	C'_{var}	var'u'	$C'_{var.u}$
v^{*2}	+ 88	0	v'^2	+ 88	v'^2u'	0
r^{*2}	0	0	r'^2	0	r'^2u'	0
δ^2	0	-177	δ^2	- 125	δ^2u'	-112
v^*r^* [1)]	+2149	0	v'r' [1)]	+2149	v'r'u'	0
$r^*\delta$	- 50	0	r'δ	- 50	r'δu'	- 50
δv^*	+ 117	0	δv'	+ 117	δv'u'	+117
$L\dot{u}/U_x^2$ [1)]	-1329	0	$\dot{u}'$ [1)]	-1329	$\dot{u}'u'$	0
resistance - and thrust coefficients						
X^*_R	- 54		u'	- 133	u'u'	- 54
X'_T	- 25					

[1)] These coefficients include the ship's mass m'

Table 10 Longitudinal Force Coefficients

4 Computer Programs

4.1 Least Squares Analysis of Measured Data

The IBM 360/65 computer program SBSL#M03 has been developed to compute the coefficients of a fourth order polynomial of four variables:

$$F(x_1, x_2, x_3, x_4) = \sum_{t=1}^{p} C_t \cdot x_1^{\,k} x_2^{\,l} x_3^{\,m} x_4^{\,n}$$

using the least square criterion. Herein is $p \le 70$ and $k + l + m + n \le 4$.

If some of the coefficients are already known they can be given and the corresponding terms are subtracted from the measured value of the function. If the distance between a measurement and the computed value of the polynomial exceeds two times the RMS value the data concerned are dropped while the coefficients are computed again. This “data point selection procedure” primarily serves to locate measuring, writing or typing errors. The factor 2 used in this criterion has been found experimentally. In statistics, usually a factor 3 is applied, though it has been found that if the number of measurement is relatively small even large errors are not located in that case.

This data point selection procedure comes into operation again, unless:

a. the number of selected data exceeds ten percent of the total number,
b. the RMS value is already smaller than a boundary value given beforehand.

In the next stage the maximum value of each term is computed. If these maximum contributions of a number of terms is smaller than the boundary value just mentioned the procedure is repeated, though without the coefficient the maximum contribution of which was the smallest.
Also this "coefficients selection procedure" is repeated until the contributions of all terms remained are sufficient.
Further the standard deviation and the correlation coefficient of each coefficient are computed. The first quantity is plotted in Figure 37 and Figure 38 concerning the large and the small model respectively.
A later version of this program can be found at the Internet: http://www.shipmotions.nl.

4.2 Solution of Differential Equations

In the IBM 360/65 computer program SBSL#M02, the differential equations are solved for given time depending rudder signals, where the Runge-Kutta procedure is applied. Two cases are considered. In the first the rudder rate is constant or zero, while in the second sinusoidal rudder input can be given to determine the frequency characteristics of a ship.
The output quantities can also be required to obtain the input for the coefficients program M03, to determine the coefficients of a mathematical model with a reduced number of coefficients. Further for each step the value of each term of the set of equations of motion is computed which enables to get an insight in the importance of the various components. An illustration of this is given in Figure 39, Figure 40 and Figure 41.

Another way to observe the process of a manoeuvre is to linearise the equations of motion at each step to the set:

$$\Delta\dot{v} = a_{11}\cdot\Delta v + a_{12}\cdot\Delta r + a_{13}\cdot\Delta d + a_{14}\cdot\Delta u$$
$$\Delta\dot{r} = a_{21}\cdot\Delta v + a_{22}\cdot\Delta r + a_{23}\cdot\Delta d + a_{24}\cdot\Delta u$$
$$\Delta\dot{u} = a_{31}\cdot\Delta v + a_{32}\cdot\Delta r + a_{33}\cdot\Delta d + a_{34}\cdot\Delta u$$

Using the coefficients of this set of equations the stability of the system can be observed. The time constants of the system can be found from the roots of the set:

$$\begin{vmatrix} a_{11}-l & a_{12} & a_{14} \\ a_{21} & a_{22}-l & a_{24} \\ a_{31} & a_{32} & a_{34}-l \end{vmatrix} = 0$$

An example of the change of these constants, indicating the change of stability, during a turning circle manoeuvre, is given in Figure 42.

Concerning the time interval between two steps of the computation, for all manoeuvres 10 steps per ship length, based on the initial speed, was applied. The time intervals following from this are given in Table 11.

U_o m/sec	Δt (sec)
8.0	2.7625
6.8	3.2500
5.6	3.9464
4.8	4.6041
3.2	6.9063
($U_o \Delta t/L$ = .100)	

Table 11 Time Intervals

5 Comparison of Computed and Full-Scale Manoeuvres

5.1 Turning Circles

The principal data of the turning circles are summarised in Table 12.

TURNING CIRCLE DATA			
nr.	9A	9B	9D2
δ_o(degr)	- 34.0	+ 37.0	- 19.0
rpm	100.0	100.0	100.0
U_o(m/sec)	8.00	8.00	8.00
β(o)(degr)	- .358	+ .358	+ .358
ψ(o)(degr)	- .858	+ .758	- .442
x_o(o)(m)	0	- .06	+ .09
y_o(o)(m)	+ .03	+ .03	+ .37
$\dot{\psi}$(o)(degr/sec)	+ .10	- .20	+ .05
δ (")	2.500	2.500	2.500

Table 12 Turning Circle Data

The results of the computed turning circles are shown in Figure 43 through Figure 46. As follows from these figures, the (final) rates of turn are somewhat smaller than the full-scale values though, combined with the final speed, the turning diameters agree very well however.
For comparison with the spiral manoeuvre results some additional turning circles have been computed. Only the final values of the various quantities have been used to obtain complete curves.
The computation of the 37 degrees port rudder turning circle has been repeated omitting certain coefficients, which significance was very little, according to the model tests. The results are shown in Figure 45. As appears from this figure these coefficients have also little importance in the mathematical model.

Table XIV. Zig-zag trial data

initial conditions				I			II			III			IV			V			VI		
nr.	rpm	U_0 (m/s)	ψ (degr)	$\dot{\delta}$ (degr/sec)	δ_0 (degr)	ψ_{ex} (degr)	$\dot{\delta}$ (degr/sec)	δ_0 (degr)	ψ_{ex} (degr)	$\dot{\delta}$ (degr/sec)	δ_0 (degr)	ψ_{ex} (degr)	$\dot{\delta}$ (degr/sec)	δ_0 (degr)	ψ_{ex} (degr)	$\dot{\delta}$ (degr/sec)	δ_0 (degr)	ψ_{ex} (degr)	$\dot{\delta}$ (degr/sec)	δ_0 (degr)	ψ_{ex} (degr)
7A	97.5	7.80	−2.6	2.708 [1]	19.0	−20.8	3.105	−19.0	14.2	3.850	18.2	−19.6	3.482	−19.2	19.9	3.591	18.6	−18.6	3.482	−19.3	9.5
7C	97.2	7.78	− .4	2.500	8.9	−15.7	2.375	− 9.7	23.2	2.436	8.8	−17.2	2.632	− 9.9	22.4						
7D	98.1	7.85	0	2.982	29.3	−16.9	3.929	−31.0	21.1	4.522	28.5	−16.1	3.719	−31.3	21.5	4.000	29.2	−16.2	3.067	−31.0	2.5
7E	87.0	6.96	0	1.020	9.5	−22.8	1.681	−10.1	23.5	1.887	9.3	−23.0	2.330	−10.3	24.0	1.944	9.3	−17.8	2.143	−10.2	20.0
7F	87.0	6.96	0	2.635	19.1	−16.7	3.565	−19.3	20.7	4.149	18.7	−16.0	3.023	−19.9	16.1	4.115	18.4	−16.2	3.185	−19.4	20.0
7G	86.4	6.91	0	2.305	29.6	−19.5	3.041	−31.3	19.5	4.020	29.2	−19.7	3.400	−30.9	20.1	4.727	28.7	−14.3	3.199	−30.9	20.0
7J	67.5	5.40	− .5	2.232	18.8	−20.0	2.950	−19.2	19.2	2.875	18.7	−19.8	3.231	−19.5	22.9	2.980	18.8	−19.2	2.760	−19.2	20.0
7L	59.7	4.78	− .7	3.488	29.3	−20.8	4.050	−30.2	19.7	4.997	28.8	−22.0	4.173	−30.5	19.5	4.355	28.8	−20.6	4.539	−30.2	0

[1]) The manoeuvres concerned have been computed with the accuracy of these data given here.

5.2 Zig-Zag Trials

In Table 13, the principal data of the zig-zag trials are summarised. Concerning the initial conditions, only the course y was considered while no other data were available. The values of the rudder rate of turn were derived from the data and figures given by Clarke (1965).

The computed zig-zag manoeuvres are plotted in Figure 47 through Figure 54 and compared with the full-scale measurements. The over-swinging angles are somewhat smaller, but the mean period-times agree very well. These two quantities are plotted in Figure 56.
Concerning the initial speed conditions of these manoeuvres the adopted linear relation: U_0 = 12.5 x rpm has been applied, while the rpm values for both full-scale trials and computations are the same.

6 Final Remarks

To judge the result of the model experiments discussed in this paper, Figure 55 and Figure 56 may serve in the first place. They provide an overall picture of the principal parameters of turning circle, spiral and zig-zag trials:

Figure 55a: r_c^* against d_0	relation between turning circle diameter ($1/r_c^*$) and rudder angle.
Figure 55b: U_c against d_0	final speed reduction of turning circle manoeuvres.
Figure 56a: t_p against $1/U_0$	relation between periods of zig-zag trial and initial speed.
Figure 56b: $y_{\max}/d_0$ against $1/d_0$	relation between over-swinging angle and nominal rudder angle.

From these figures, in which the computed quantities are compared with those measured during the full-scale trials, it appears that it is possible to predict the manoeuvring properties of the ship concerned by means of oscillation tests with reasonable accuracy.
It must be noted however that both full-scale data and computed data have their uncertainties. In particular this may be important if x_0, y_0 plots are compared, because these plots are obtained very indirectly.
Concerning the zig-zag trials it is found that a little change of the “execution course” has a relatively large effect on the maximum course deviation and the period time. Finally we have to keep in mind that the determination of the manoeuvring properties of a ship via horizontal oscillation tests is rather indirect, at least while the motions of the model during these tests are rather unrealistic. From the four figures above mentioned, it may then be concluded that if scale effects play a role in the present investigation their importance is not very large and of the same magnitude as the accuracy of both the full-scale and model-scale measurements.

6 Recommendations

The mathematical description of the manoeuvring properties is based on a hypothesis, which describes the relation between the forces acting on the ship and the forward speed. The

application of this hypothesis is fully justified by the present model experiments. This does not mean however that all hydrodynamic effects, which play a part in this mathematical model, are really necessary for a sufficient description of the horizontal motions. Therefore, it might be interesting to find a simple mathematical model, which properties are not to give and accurate description of the hydrodynamic phenomena but rather of the motions.

8 Appendix: Relation between Second Order Similarity Parameters and Velocities and Accelerations

The second order similarity parameters are:

$$\frac{\partial x_0^*}{\partial s^*}, \frac{\partial y_0^*}{\partial s^*}, \frac{\partial y}{\partial s^*}, \frac{\partial t^*}{\partial s^*}, \frac{\partial^2 x_0^*}{\partial s^{*2}}, \frac{\partial^2 y_0^*}{\partial s^{*2}}, \frac{\partial^2 y}{\partial s^{*2}} \text{ and } \frac{\partial^2 t^*}{\partial s^{*2}}.$$

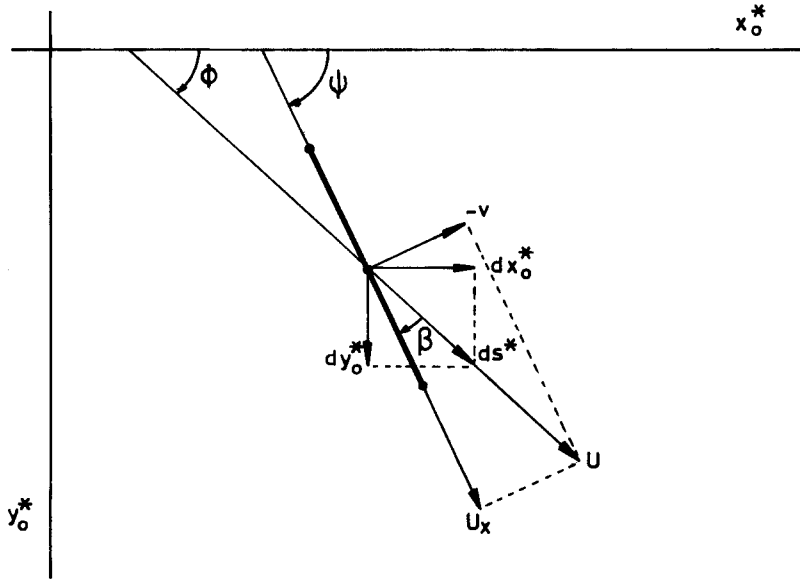

Choosing the co-ordinate system at the moment of comparison in such a way that

$$y_1 = y_2 \tag{1}$$

then from the equality of $\frac{\partial x_0^*}{\partial s^*}$ and that of $\frac{\partial y_0^*}{\partial s^*}$ it follows that:

$$f_1 = f_2 \tag{2}$$

so that also:

$$b_1 = b_2 \tag{3}$$

As:

$$\frac{v}{U} = -\sin b \tag{4}$$

from (3) it follows that:

$$\frac{v_1}{U_1} = \frac{v_2}{U_2} \tag{5}$$

From the equality of $\frac{\partial y}{\partial s^*}$ and that of $\frac{\partial^2 x_0^*}{\partial s^{*2}}$ (and $\frac{\partial^2 y_0^*}{\partial s^{*2}}$) it follows that:

$$\frac{\partial b_1}{\partial s^*} = \frac{\partial b_2}{\partial s^*} \tag{6}$$

From the equality of $\frac{\partial t^*}{\partial s^*}$ it follows that:

$$\frac{1}{T_1} \cdot \frac{\partial t_1}{\partial s^*} = \frac{1}{T_2} \cdot \frac{\partial t_2}{\partial s^*} \tag{7}$$

and because:

$$\frac{T_1}{T_2} = \frac{U_2 \cdot L_1}{U_1 \cdot L_2} \tag{8}$$

it follows from the equality:

$$\frac{\partial y_1}{\partial s^*} = \frac{\partial y_2}{\partial s^*} \tag{9}$$

that:

$$\frac{L_1 \cdot \dot{y}_1}{U_1} = \frac{L_2 \cdot \dot{y}_2}{U_2} \tag{10}$$

From equality (6), together with the equalities (7), (8), (4) and (5), it follows that:

$$\frac{L_1 \cdot \dot{v}_1}{U_1^2} - \frac{v_1}{U_1} \cdot \frac{L_1 \cdot \dot{U}_1}{U_1^2} = \frac{L_2 \cdot \dot{v}_2}{U_2^2} - \frac{v_2}{U_2} \cdot \frac{L_2 \cdot \dot{U}_2}{U_2^2} \tag{11}$$

From the equality of $\frac{\partial^2 y}{\partial s^{*2}}$, together with the equalities (7) and (8), it follows that:

$$\frac{L_1^2 \cdot \dot{r}_1}{U_1^2} - \frac{L_1 \cdot r_1}{U_1} \cdot \frac{L_1 \cdot \dot{U}_1}{U_1^2} = \frac{L_2^2 \cdot \dot{r}_2}{U_2^2} - \frac{L_2 \cdot r_2}{U_2} \cdot \frac{L_2 \cdot \dot{U}_2}{U_2^2} \tag{12}$$

where $\frac{\partial y}{\partial t}$ and $\frac{\partial^2 y}{\partial t^2}$ are denoted as r and $\dot{r}$, respectively.

From the equality of $\frac{\partial^2 t^*}{\partial s^{*2}}$, together with (7) and (8), it follows that:

$$\frac{L_1 \cdot \dot{U}_1}{U_1^2} = \frac{L \cdot \dot{U}_2}{U_2^2} \tag{13}$$

so that from equalities (11) and (12) it follows that:

$$\frac{L_1 \cdot \dot{v}_1}{U_1^2} = \frac{L_2 \cdot \dot{v}_2}{U_2^2} \quad \text{and} \quad \frac{L_1^2 \cdot \dot{r}_1}{U_1^2} = \frac{L_2^2 \cdot \dot{r}_2}{U_2^2} \tag{14}$$

Further, the equalities (5), (10), (11) and (12) are defined as follows:

$$(5): \quad v_1^* = v_2^*$$
$$(10): \quad r_1^* = r_2^*$$
$$(11): \quad \dot{v}_1^* = \dot{v}_2^*$$
$$(12): \quad \dot{r}_1^* = \dot{r}_2^*$$

Summarising, we can state that provided two conditions of motion instantaneously satisfy a second order similarity; this is equivalent to the equality:

$$v^*,\ r^*,\ \frac{L \cdot \dot{v}}{U^2},\ \frac{L^2 \cdot \dot{r}}{U^2} \text{ and } \frac{L \cdot \dot{U}}{U^2} \text{ respectively}$$

Finally, some definitions and relations between variables, which clarify their physical meaning:

$$r^* = \frac{\partial y}{\partial s^*}$$
$$\dot{v}^* = \frac{\partial v^*}{\partial s^*}$$
$$\dot{r}^* = \frac{\partial r^*}{\partial s^*}$$

$$\frac{L}{R_r} = \frac{\partial y}{\partial s^*} = r^*$$ R_r : "yaw-radius" of curvature

$$\frac{L}{R_v} = \frac{\partial b}{\partial s^*}$$ R_v : "drift-radius" of curvature

$$\frac{L}{R} = \frac{\partial f}{\partial s^*} = \frac{L}{R_r} - \frac{L}{R_v}$$ R : radius of curvature

$$\frac{\partial(-\sin b)}{\partial s^*} = \dot{v}^*$$
$$\frac{\partial(L / R_r)}{\partial s^*} = \frac{\partial^2 y}{\partial s^{*2}} = \dot{r}^*$$

9 List of Symbols

m	Mass of the ship
I_{zz}	Moment of inertia of the ship
r	Density of water
x_0, y_0	Co-ordinates in space bounded co-ordinate system
Y	Lateral force, positive to starboard
N	Moment around z_0-axis, positive to the right
X	Longitudinal force
$Y_{\dot{v}}$	Added mass in lateral direction
$N_{\dot{r}}$	Added moment of inertia

$X_{\dot{u}}$	Added mass in longitudinal direction
$Y_{a,1,2}, N_{a,1,2}, X_{1,2,3}$	Components of Y, N and X respectively
$\overline{Y}_2, \overline{N}_2, \overline{X}_2$	Components proportional to $U_R^{\ 2}$
$X_R^{\ '}$	Thrust increment coefficient
$X_R^{\ *}$	Longitudinal resistance coefficient
$Y_1^{\ *}$	$= \dfrac{Y_1}{\frac{1}{2} r U^2 L^2} \approx \dfrac{Y_1}{\frac{1}{2} r U_x^{\ 2} L^2}$
$N_1^{\ *}$	$= \dfrac{N_1}{\frac{1}{2} r U^2 L^3} \approx \dfrac{N_1}{\frac{1}{2} r U_x^{\ 2} L^3}$
$X_1^{\ *}$	$= \dfrac{X_1}{\frac{1}{2} r U^2 L^2} \approx \dfrac{X_1}{\frac{1}{2} r U_x^{\ 2} L^2}$
U_0	Initial speed
U, $\dot{U}$	Instantaneous forward speed and acceleration (vector)
U_x, $\dot{U}_x$	Instantaneous longitudinal speed and acceleration
U_R	Local velocity near the rudder
v, $\dot{v}$	Sway (drift) velocity and acceleration
r, $\dot{r}$	Yaw angular velocity and acceleration
d	Rudder angle
u	Speed reduction: $u = U_x - U_0$
v^*	$= v/U = -\sin b \approx v/U_x = -\tan b$
r^*	$= dy/ds^* = L \cdot r/U \approx L/R_r \approx L \cdot r/U_x$
$\dot{v}^*$	$= dv^*/ds^*$
$\dot{r}^*$	$= dr^*/ds^*$
y	Heading angle
b	Drift angle
f	Deviation angle
$\dot{f}^*$	$= df/ds^* = L/R = L/R_r - L/R_v$
s	Distance covered by the ship
s^*	Distance covered by the ship in ship lengths
R	Radius of curvature
R_v	Drift radius of curvature ($L/R_v = db/ds^*$)
R_r	Yaw radius of curvature ($L/R_r = dy/ds^*$)
$m^{'}$	$= m/0.5 r L^3$
$I_{zz}^{\ '}$	$= I_{zz}/0.5 r \mathrm{L}^5$
$v^{'}$	$= v/U_0$
$r^{'}$	$= L \cdot r/U_0$
$u^{'}$	$= u/U_0$

$$\dot{v}' = L \cdot \dot{v} / U_0^2$$
$$\dot{r}' = L^2 \cdot \dot{r} / U_0^2$$
$$\dot{u}' = L \cdot \dot{u} / U_0^2$$
$$U_R' = U_R / U_0$$

10 References

Abkowitz (1964)
M.A. Abkowitz, *Lectures on Ship Hydrodynamics - Steering and Manoeuvrability,* HyA Report HY-5, December 1964.

Clarke (1965)
D. Clarke, *Manoeuvring Trials with the 50.000 Ton Deadweight Tanker "British Bombardier"*, BSRA Report, December 1965.

Davidson and Schiff (1946)
K.S.M. Davidson and L.J. Schiff, *Turning and Course Keeping Qualities*, SNAME 1946.

Eda and Crane (1962)
H. Eda, and C.L. Crane, *Research on Ship Controllability,* D.L. Report, Stevens Institute of Technology, 1962.

Nomoto (1967)
K. Nomoto, *On the Steering Qualities of Ships*, I.S.P. July 1957.

Van Leeuwen (1964)
G. van Leeuwen, *The Lateral Damping and Added Mass of a Horizontally Oscillating Shipmodel*, T.N.O. Report 65S, December 1964.

Van Leeuwen (1969a)
G. van Leeuwen, *Enkele problemen bij het ontwerpen van een horizontale oscillator (in Dutch)*, T.H. Shipbuilding Laboratory, Report 225, January 1969.

Van Leeuwen (1969b)
Van Leeuwen, *Some Notes on the Discrepancies between the Lateral Motions of Oscillation Tests and Full-Scale Manoeuvres*, T.H. Shipbuilding Laboratory Report 232, April 1969.

Van Leeuwen (1969c)
G. van Leeuwen, *Tentative Results of the Horizontal Oscillation Tests with a 4-Meter Model of the "British Bombardier"*, T.H. Shipbuilding Laboratory, Report 239, June 1969.

Van Leeuwen (1970)
G. van Leeuwen, *A Simplified Non-Linear Model of a Manoeuvring Ship*, T.H. Shipbuilding Laboratory, Report 262, March 1970.

Zunderdorp and Buitenhek (1963)
H.J. Zunderdorp and M. Buitenhek, *Oscillator Techniques at the Shipbuilding Laboratory*, T.H. Shipbuilding Laboratory, Report 111, November 1963.

11 Figures

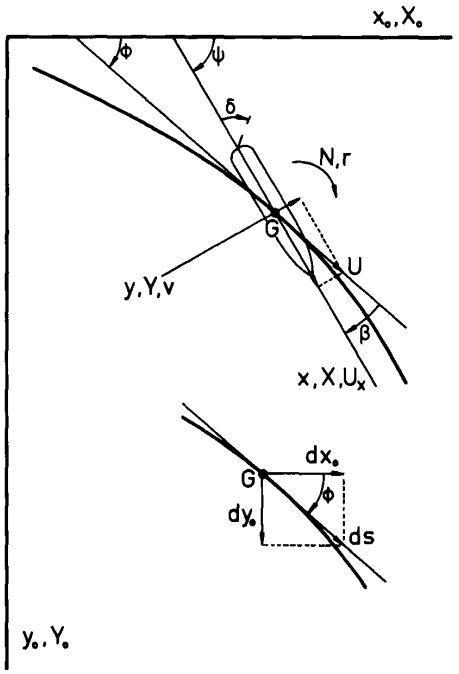

Figure 1 Co-ordinate System and Definition of Variables

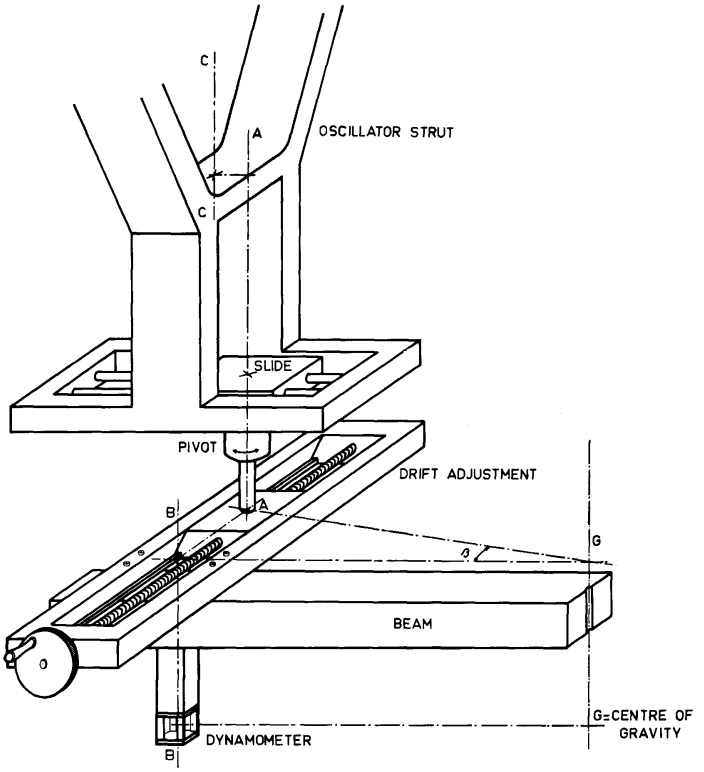

Figure 2 Drift Angle Adjustment of Oscillator

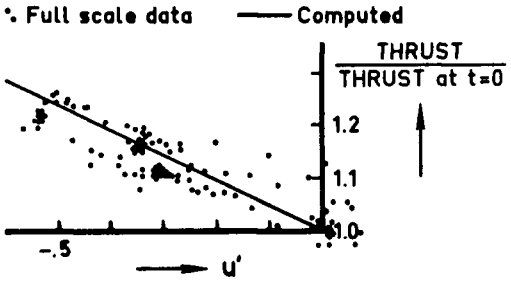

Figure 3 Variation of Thrust with Speed during Turning Circles at 100 Nominal RPM at t = 0

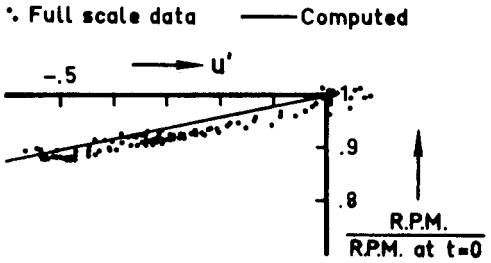

Figure 4 Variation of RPM with Speed during Turning Circles at 100 Nominal RPM at t = 0

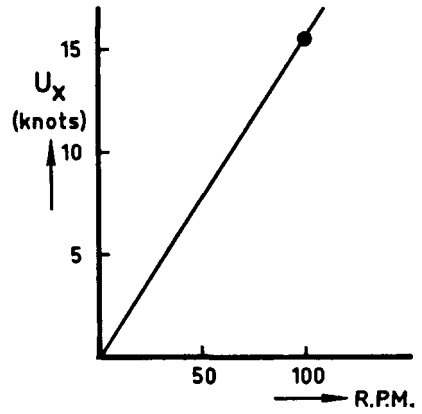

Figure 5 Adopted Initial Speed-RPM Relation

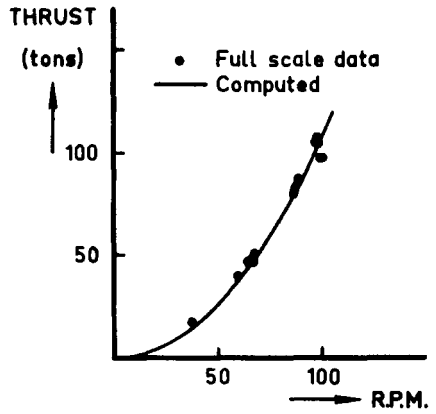

Figure 6 Measured and Computed Values of Thrust

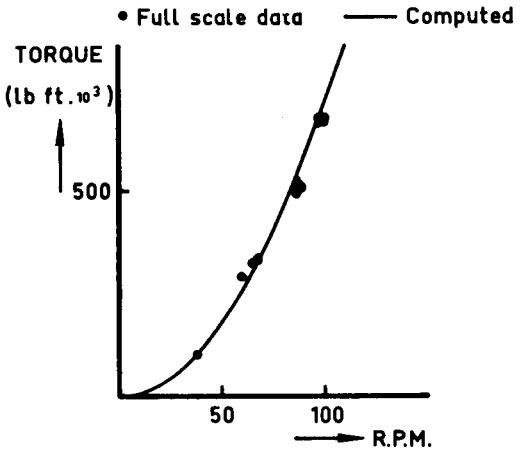

Figure 7 Measured and Computed Values of Torque

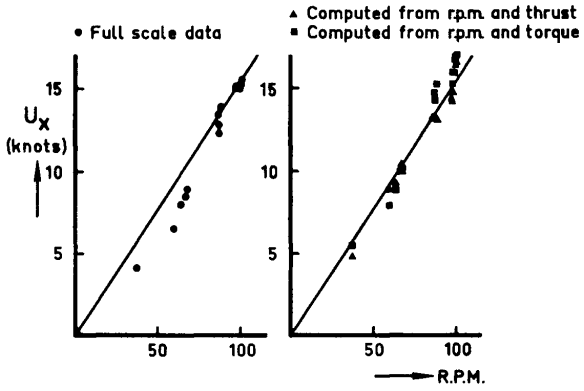

Figure 8 Discrepancies between Measured Forward Speed and Speed Derived from Thrust and Torque Measurements (Full-Scale)

U_x(m/sec)	n (r.p.s.)			
1.08	● 12.38			
.86	◐ 11.95	■ 10.29		
.65	◓ 11.54	◩ 9.85	▲ 8.34	
.43	○ 11.20	□ 9.53	△ 8.00	+ 6.50

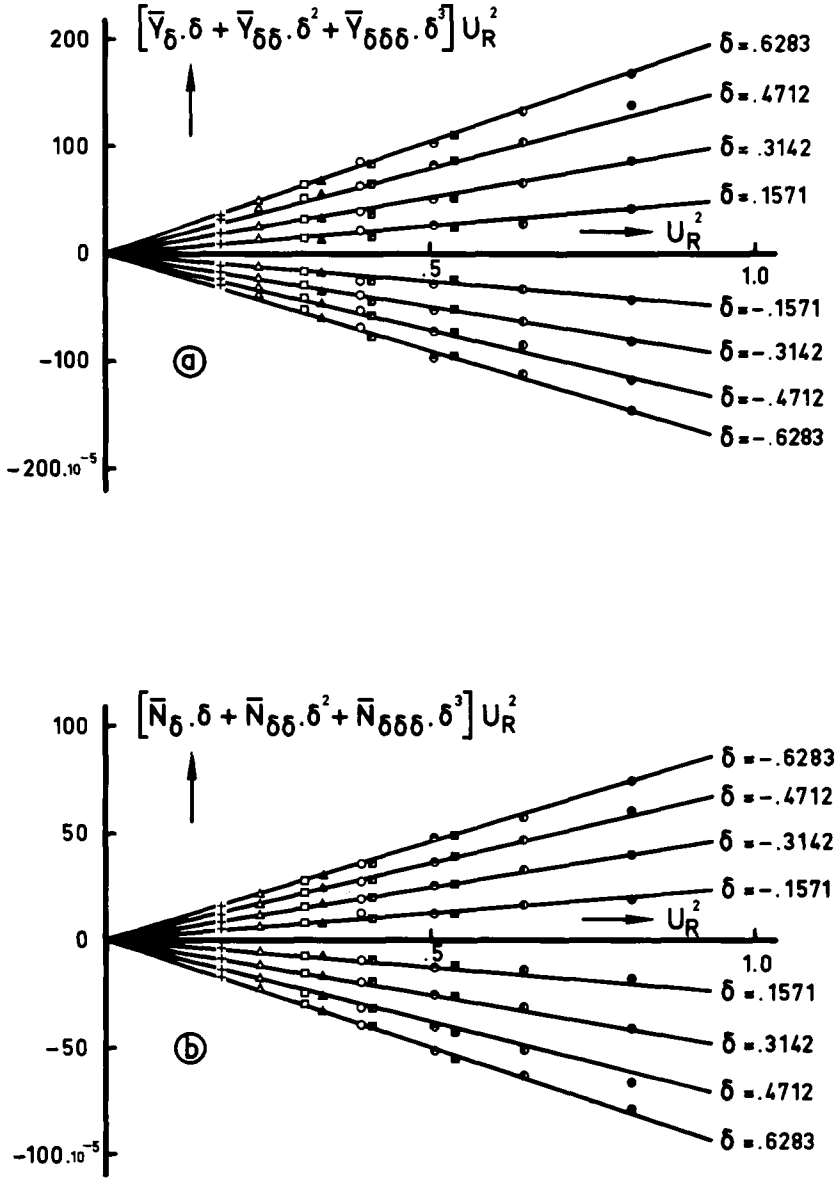

Figure 9 Lateral Force and Moment due to a Rudder Deflection

U_x (m/sec)	n (r.p.s.)			
1.08	● 12.38			
.86	◐ 11.95	■ 10.29		
.65	◓ 11.54	◩ 9.85	▲ 8.34	
.43	○ 11.20	□ 9.53	△ 8.00	+ 6.50

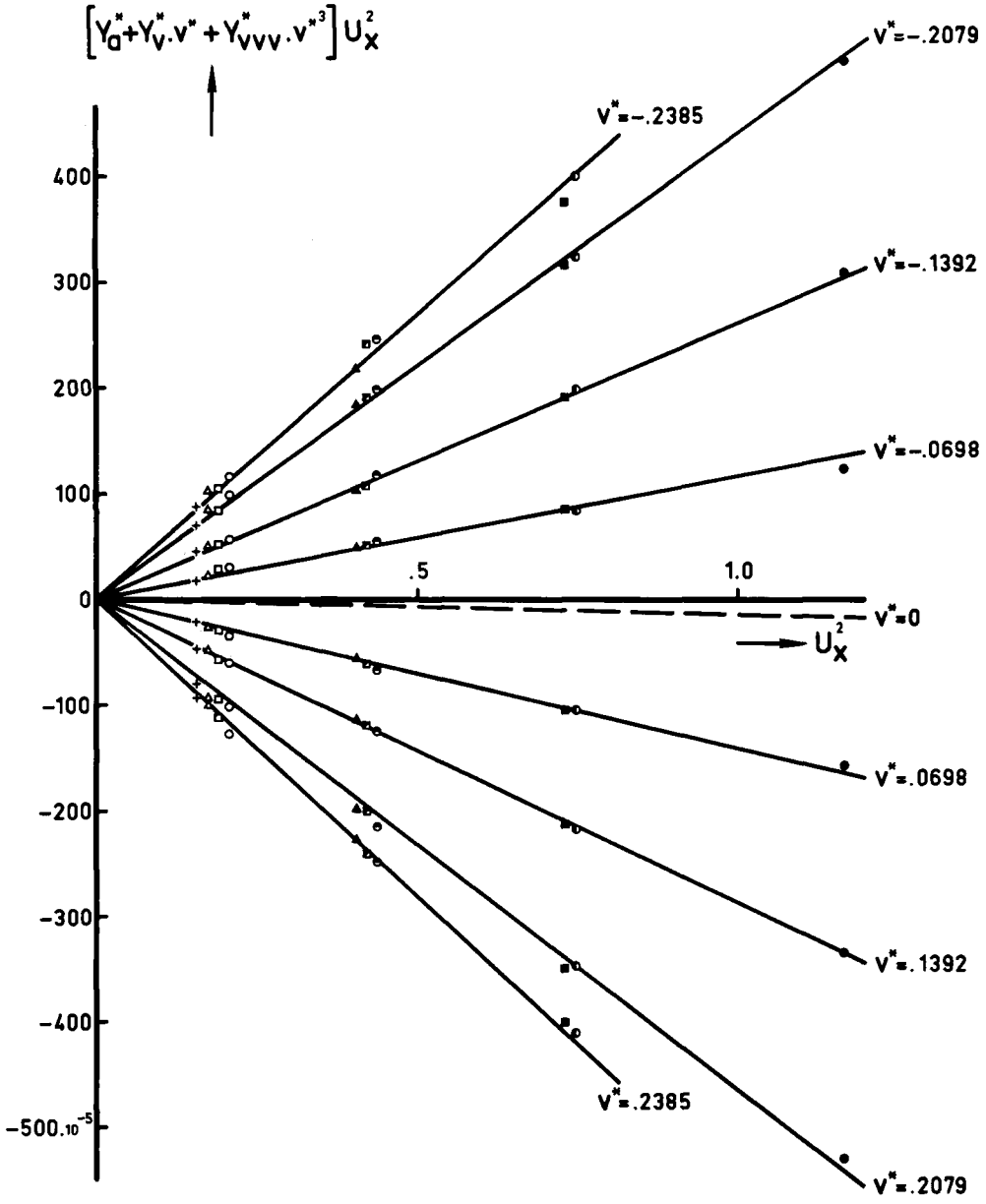

Figure 10 Lateral Sway Damping Force

U_x(m/sec)	n (r.p.s.)			
1.08	● 12.38			
.86	◐ 11.95	■ 10.29		
.65	◓ 11.54	◩ 9.85	▲ 8.34	
.43	○ 11.20	□ 9.53	△ 8.00	+ 6.50

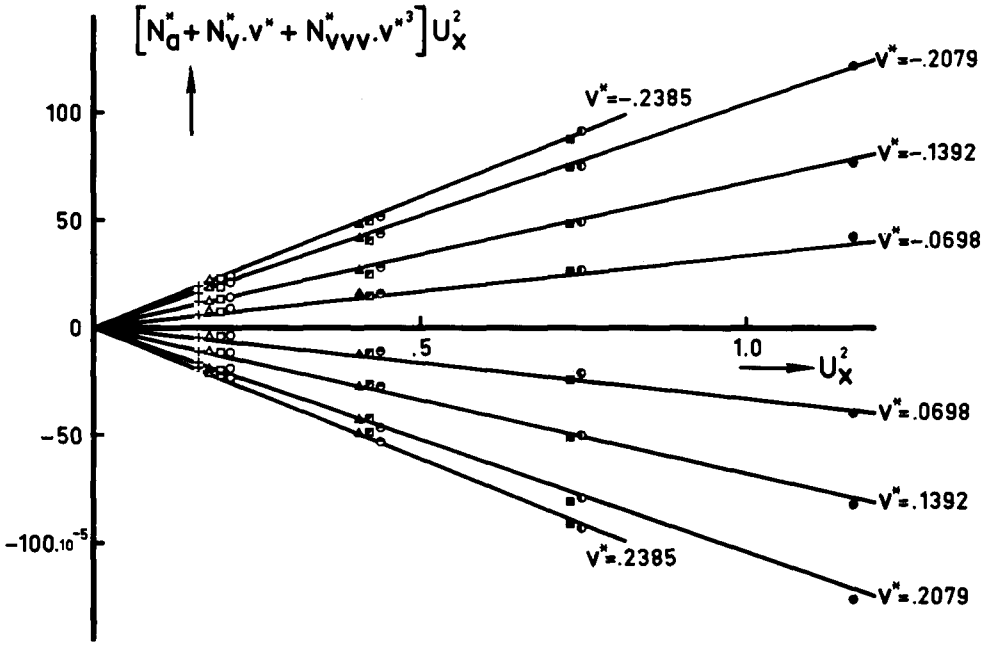

Figure 11 Lateral Sway Damping Moment

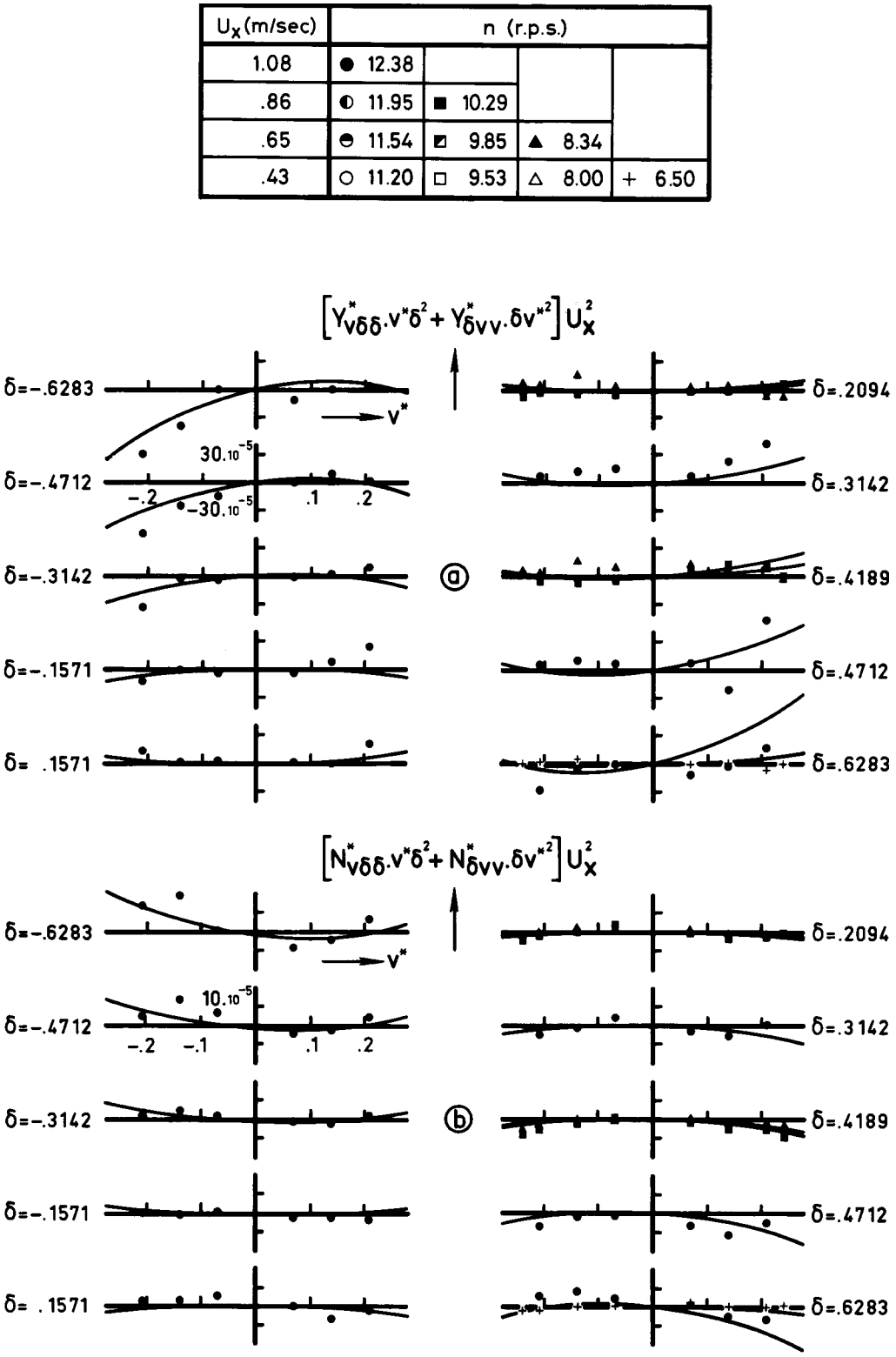

Figure 12 Rudder Angle – Drift (vd^2 and dv^2) Cross Coupling Effect in Lateral Force and Moment

U_x (m/sec)	n (r.p.s.)			
1.08	● 12.38			
.86	◐ 11.95	■ 10.29		
.65	◓ 11.54	◩ 9.85	▲ 8.34	
.43	○ 11.20	□ 9.53	△ 8.00	+ 6.50

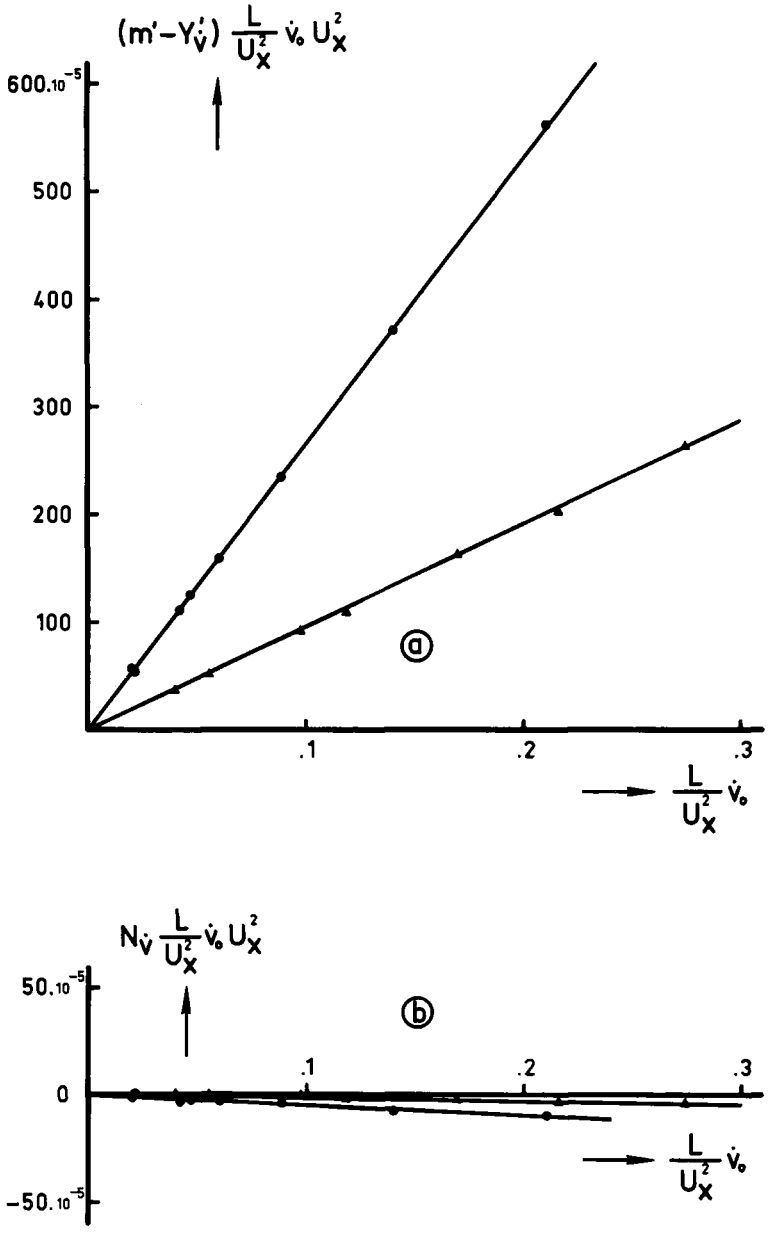

Figure 13 Sway Force and Moment due to Lateral Mass

U_x (m/sec)	n (r.p.s.)			
1.08	● 12.38			
.86	◐ 11.95	■ 10.29		
.65	◓ 11.54	◩ 9.85	▲ 8.34	
.43	○ 11.20	□ 9.53	△ 8.00	+ 6.50

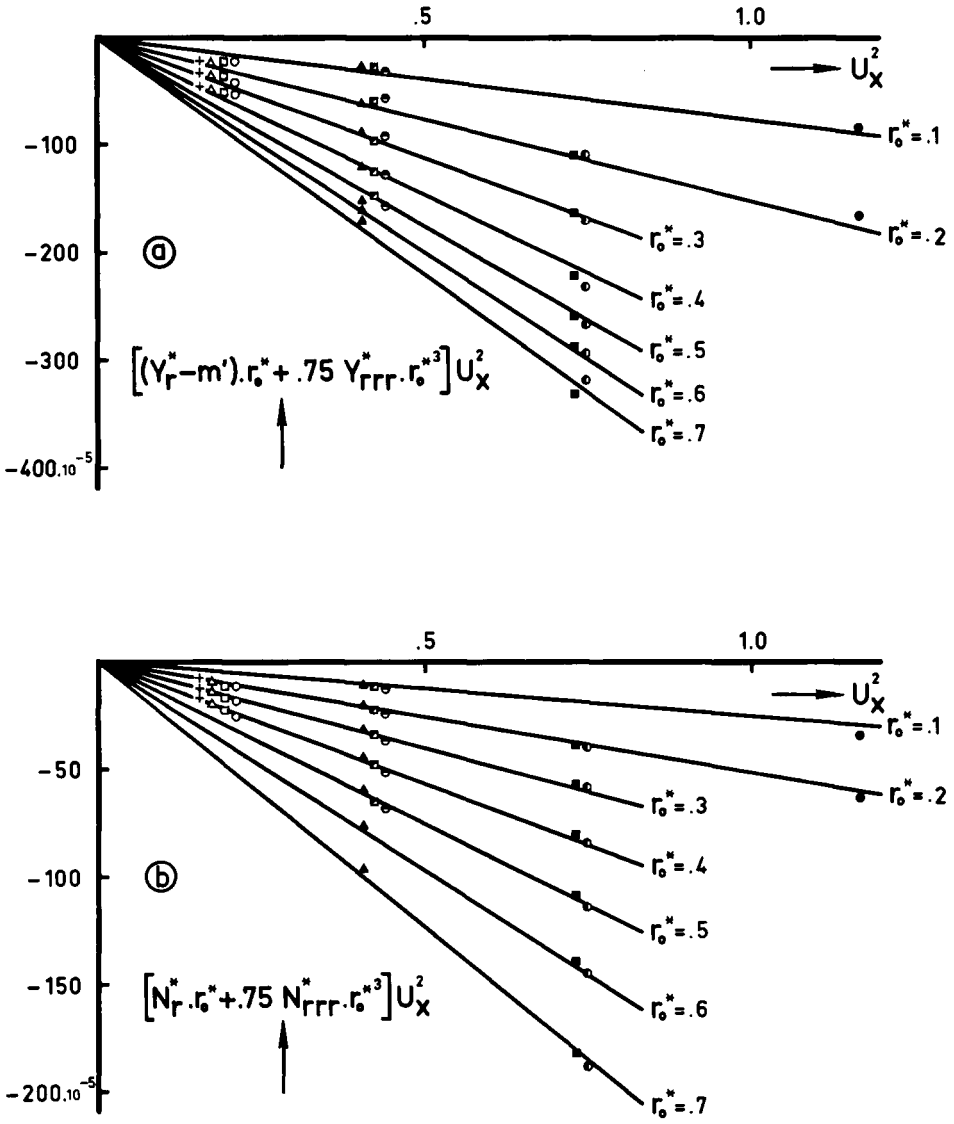

Figure 14 Lateral Yaw Damping Force and Moment

U_x (m/sec)	n (r.p.s.)			
1.08	● 12.38			
.86	◐ 11.95	■ 10.29		
.65	◓ 11.54	◪ 9.85	▲ 8.34	
.43	○ 11.20	□ 9.53	△ 8.00	+ 6.50

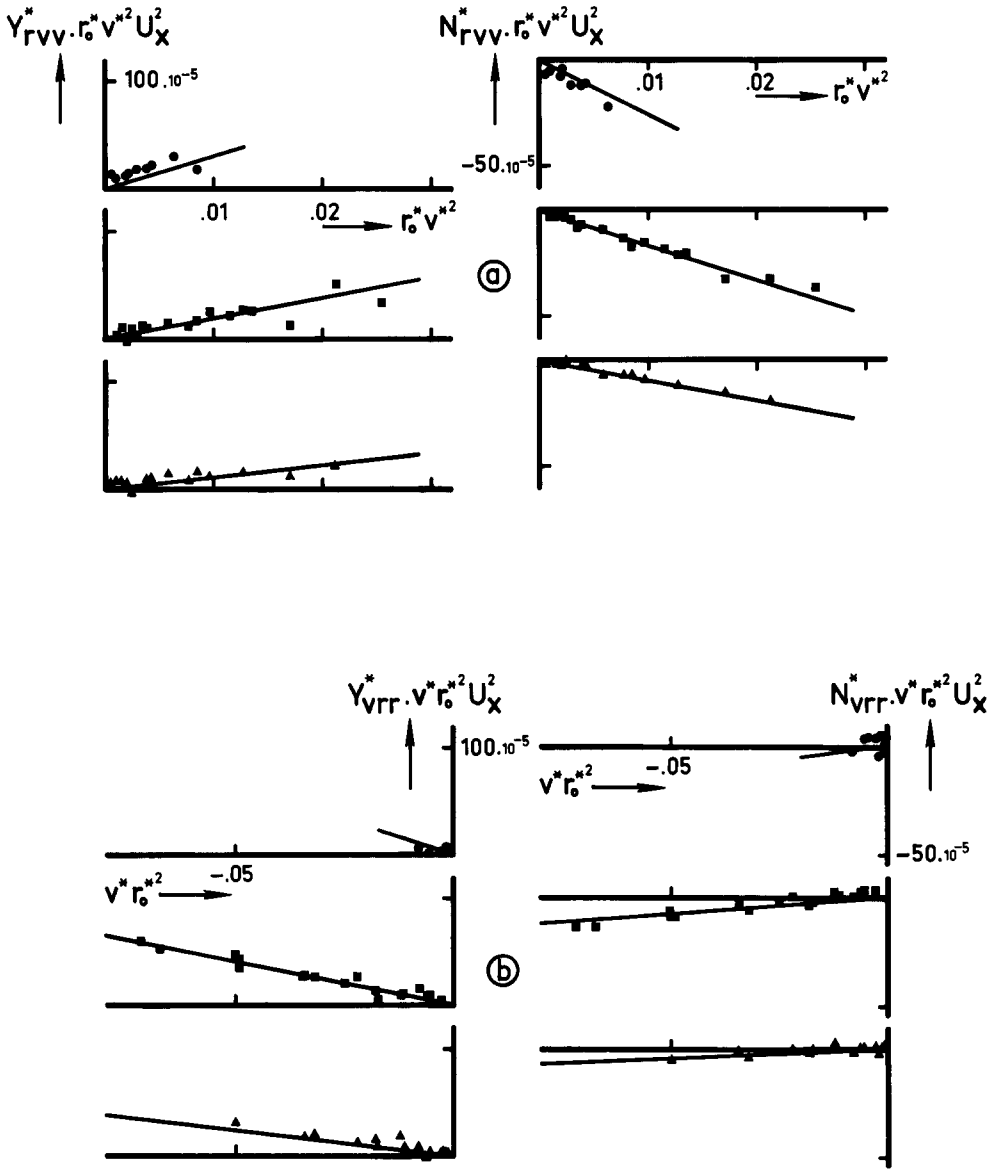

Figure 15 Yaw Rate – Drift (rv^2 and vr^2) Cross Coupling Effects in Lateral Force and Moment

U_x (m/sec)	n (r.p.s.)			
1.08	● 12.38			
.86	◐ 11.95	■ 10.29		
.65	◓ 11.54	◩ 9.85	▲ 8.34	
.43	○ 11.20	□ 9.53	△ 8.00	+ 6.50

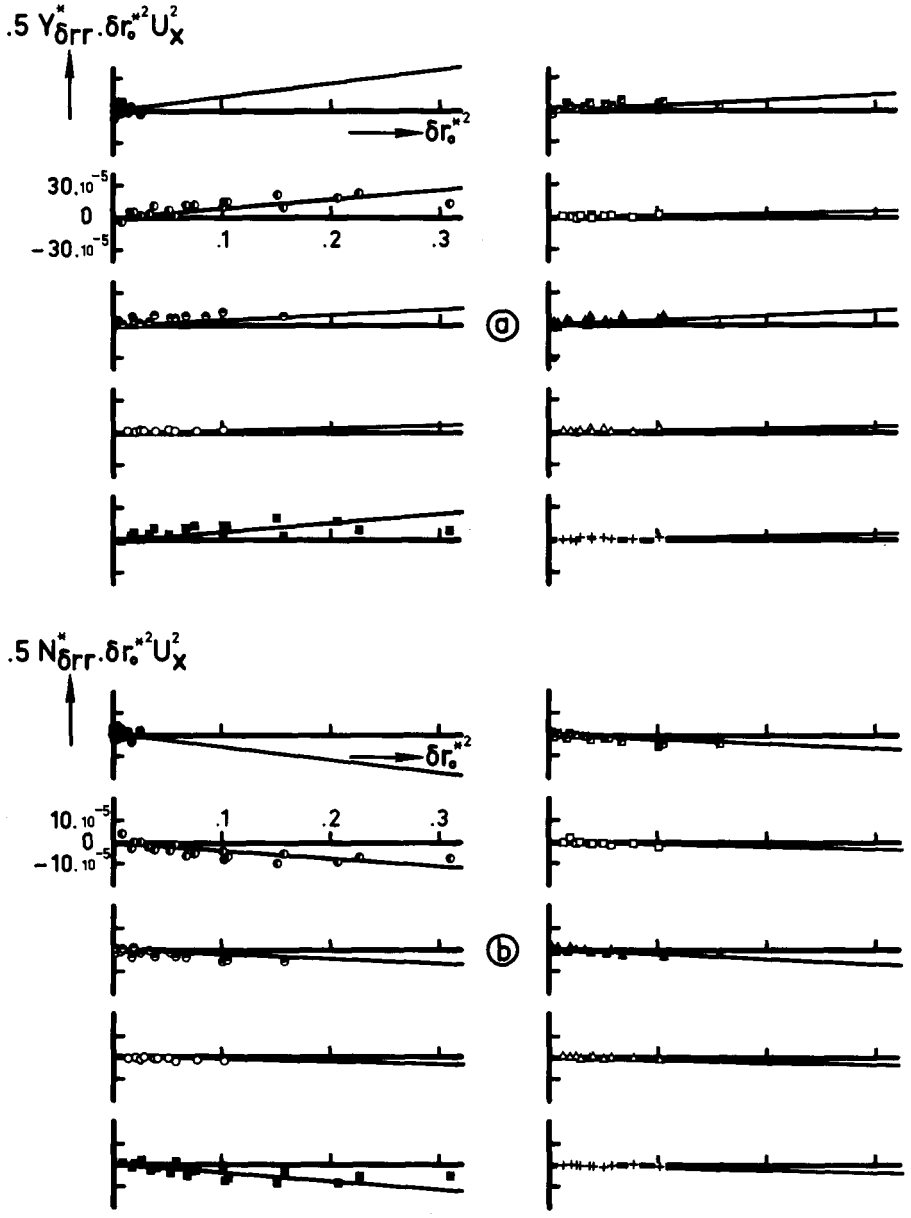

Figure 16 Rudder Angle – Yaw Rate (dr^2) Cross Coupling Effect in Lateral Force and Moment

U_x (m/sec)	n (r.p.s.)			
1.08	● 12.38			
.86	◐ 11.95	■ 10.29		
.65	◓ 11.54	◩ 9.85	▲ 8.34	
.43	○ 11.20	□ 9.53	△ 8.00	+ 6.50

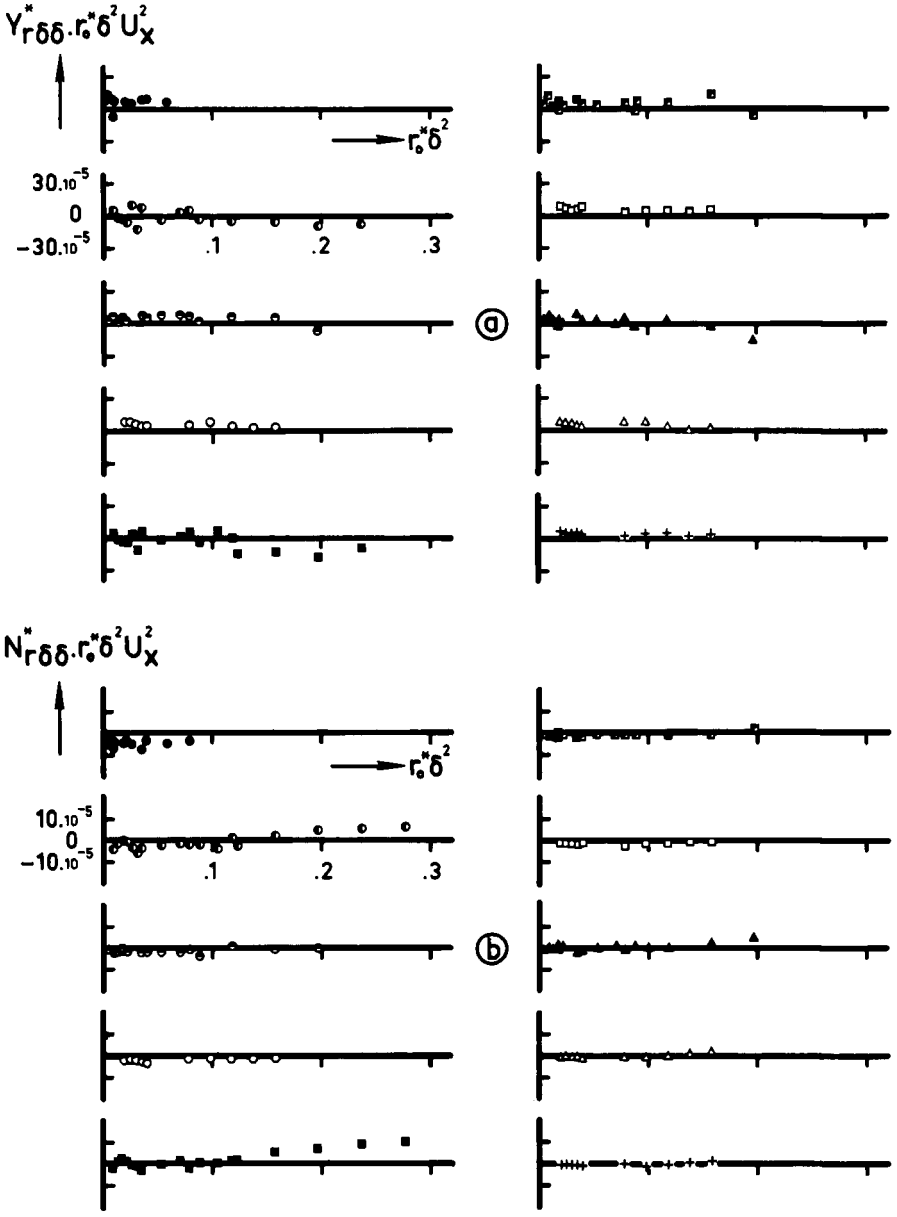

Figure 17 Yaw Rate – Rudder Angle (rd^2) Cross Coupling Effect in Lateral Force and Moment

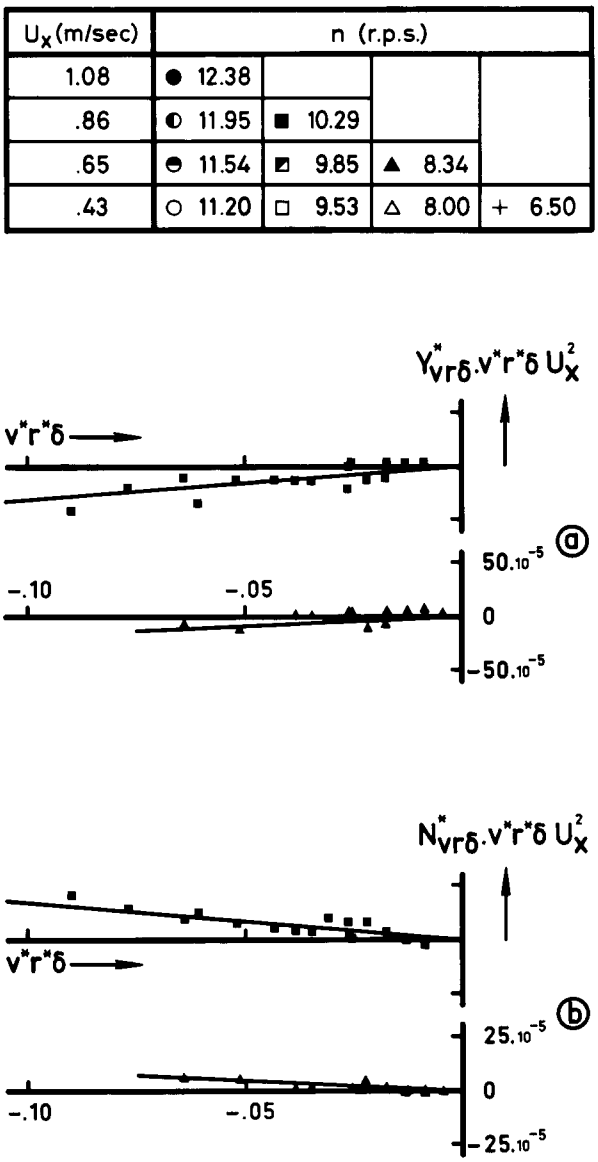

Figure 18 Drift – Yaw Rate – Rudder Angle (*vrd*) Cross Coupling Effect in Lateral Force and Moment

U_x (m/sec)	n (r.p.s.)			
1.08	● 12.38			
.86	◐ 11.95	■ 10.29		
.65	◓ 11.54	◪ 9.85	▲ 8.34	
.43	○ 11.20	□ 9.53	△ 8.00	+ 6.50

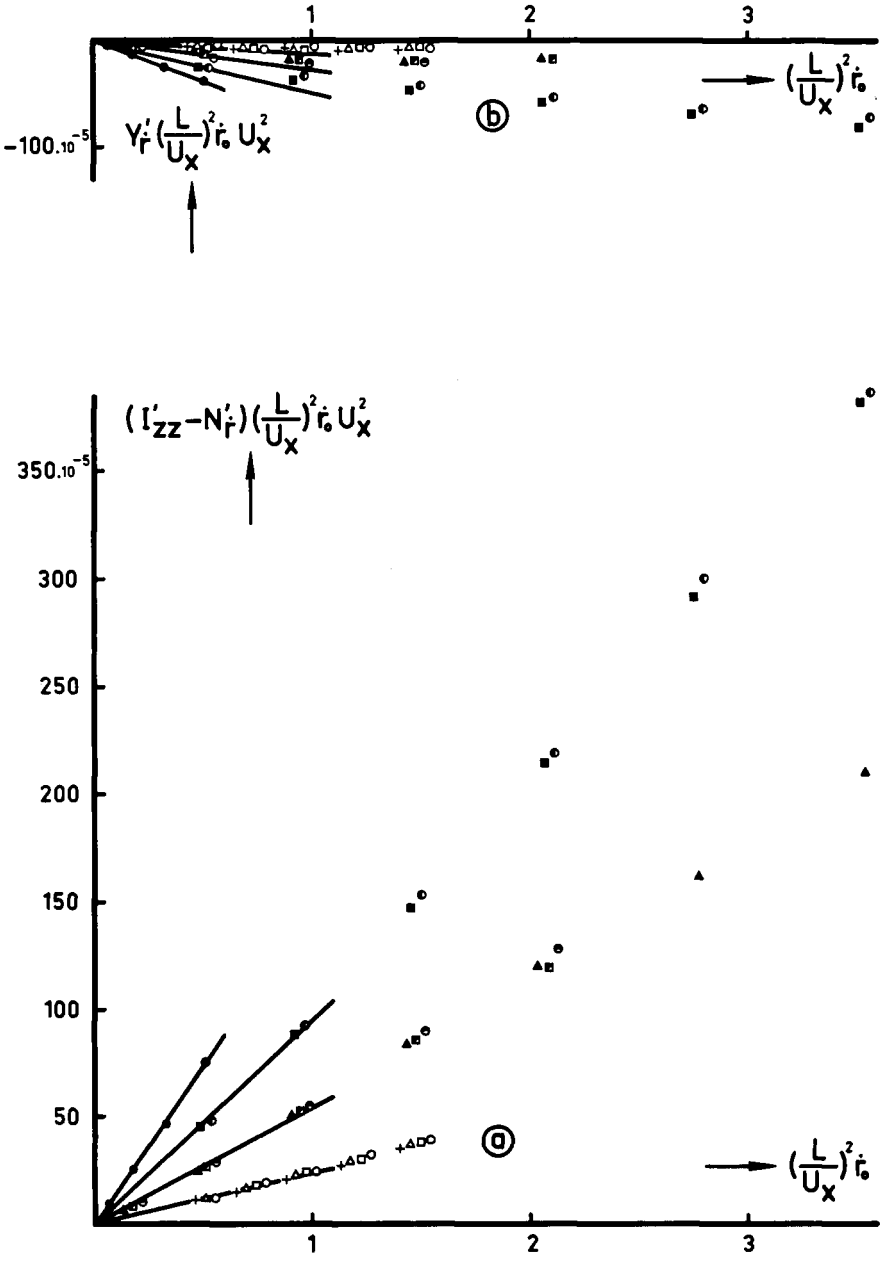

Figure 19 Yawing Force and Moment due to Moment of Inertia

U_x(m/sec)	n (r.p.s.)			
1.08	● 12.38			
.86	◐ 11.95	■ 10.29		
.65	◓ 11.54	◪ 9.85	▲ 8.34	
.43	○ 11.20	□ 9.53	△ 8.00	+ 6.50

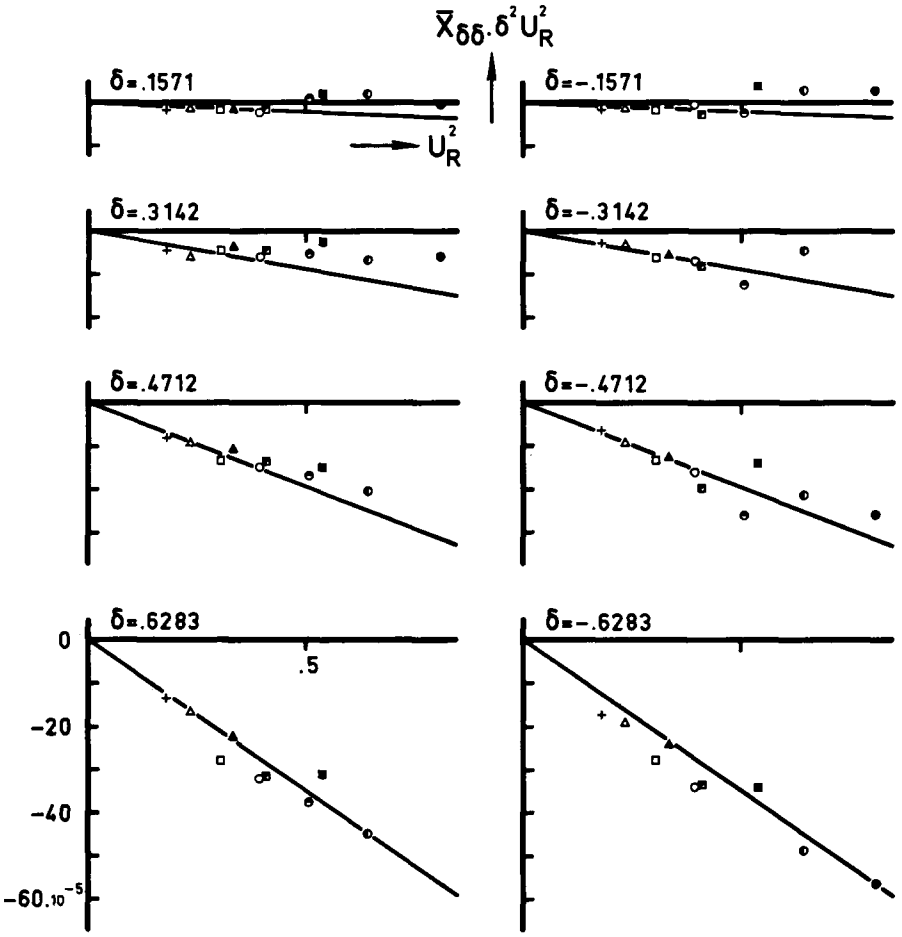

Figure 20 Longitudinal Force due to a Rudder Deflection

U_x(m/sec)	n (r.p.s.)			
1.08	● 12.38			
.86	◐ 11.95	■ 10.29		
.65	◓ 11.54	◩ 9.85	▲ 8.34	
.43	○ 11.20	□ 9.53	△ 8.00	+ 6.50

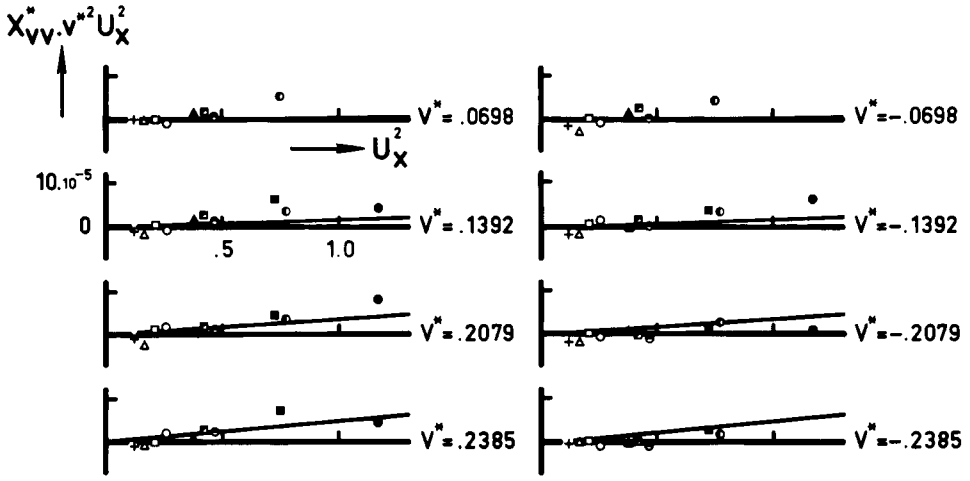

Figure 21 Longitudinal Sway Damping Force

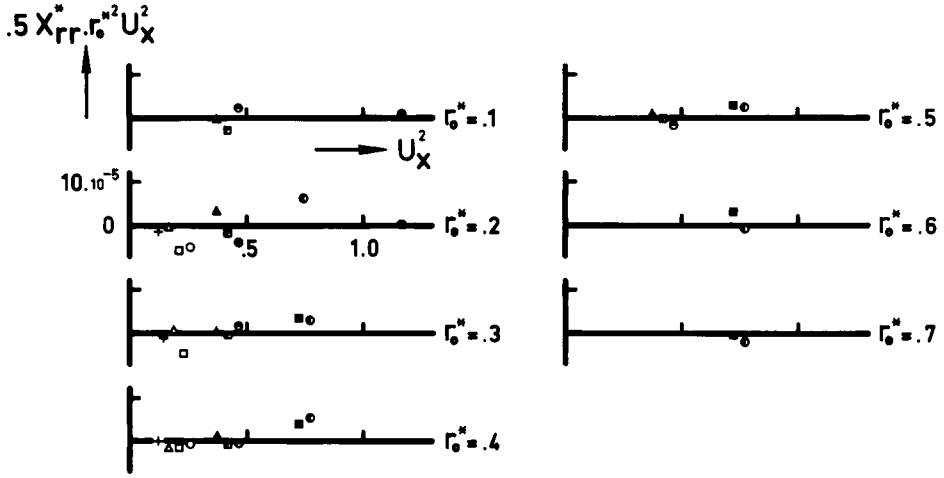

Figure 22 Longitudinal Yaw Damping Force

U_x(m/sec)	n (r.p.s.)			
1.08	● 12.38			
.86	◐ 11.95	■ 10.29		
.65	◓ 11.54	◩ 9.85	▲ 8.34	
.43	○ 11.20	□ 9.53	△ 8.00	+ 6.50

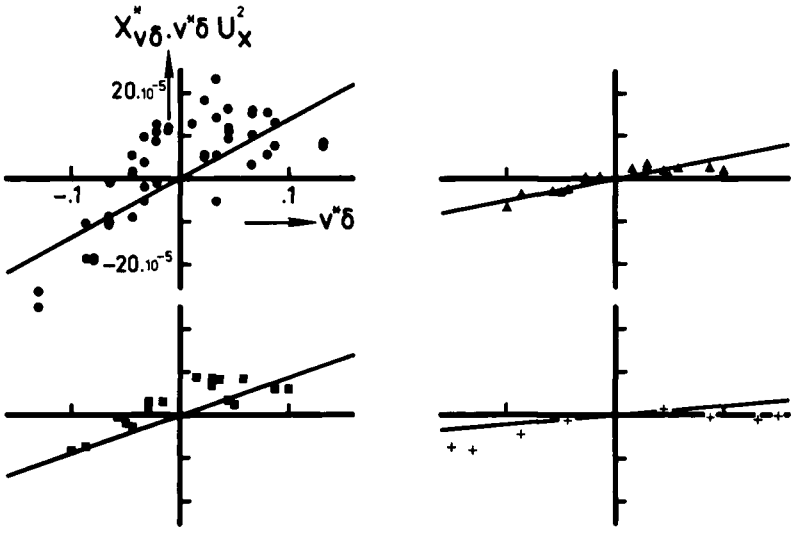

Figure 23 Rudder Angle – Drift (*vd*) Cross Coupling Effect in Longitudinal Force

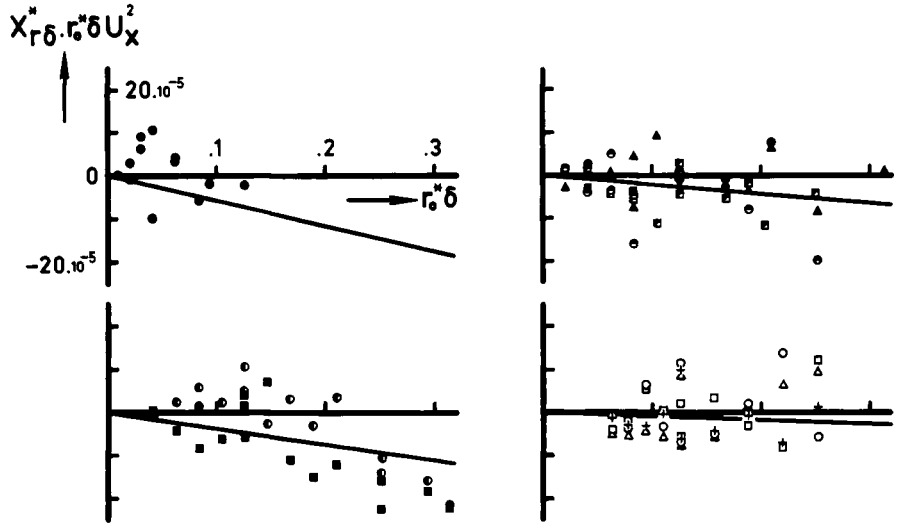

Figure 24 Rudder Angle – Yaw Rate (*rd*) Cross Coupling Effect in Longitudinal Force

U_x (m/sec)	n (r.p.s.)			
1.08	● 12.38			
.86	◐ 11.95	■ 10.29		
.65	◓ 11.54	◩ 9.85	▲ 8.34	
.43	○ 11.20	□ 9.53	△ 8.00	+ 6.50

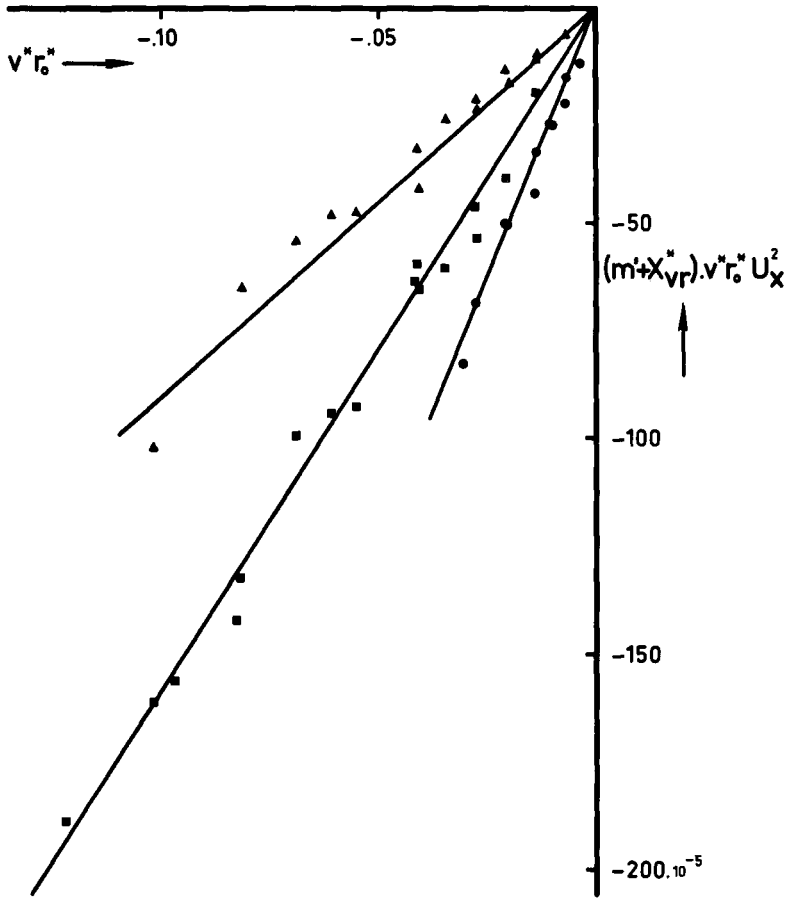

Figure 25 Longitudinal Force due to Centrifugal Acceleration

SMALL MODEL 1:100

	●	■	▲	+
U_x (m/sec)	.80	.64	.48	.32
n (r.p.s.)	16.43	13.14	9.86	6.57

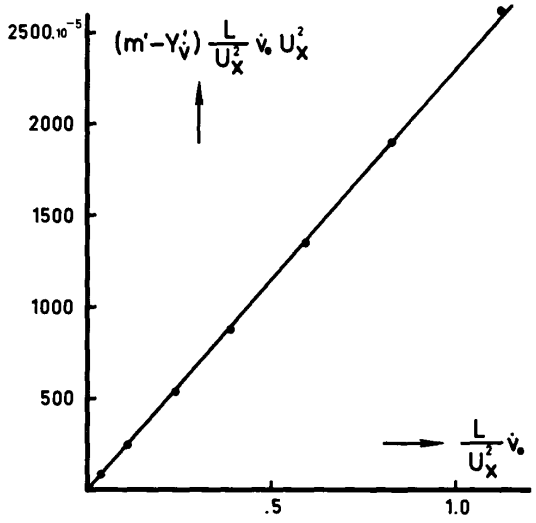

Figure 26 Swaying Force due to Lateral Mass (Small Model 1:100)

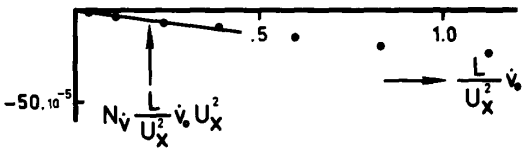

Figure 27 Swaying Moment due to Lateral Mass (Small Model 1:100)

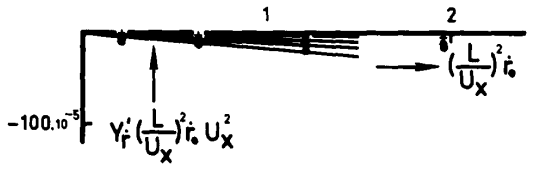

Figure 28 Yawing Force due to Moment of Inertia (Small Model 1:100)

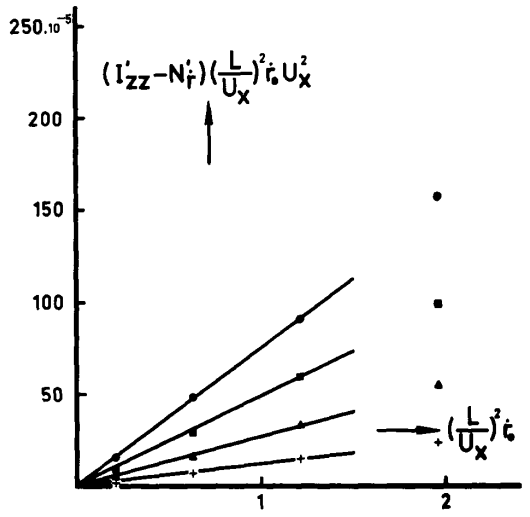

Figure 29 Yawing Moment due to Moment of Inertia (Small Model 1:100)

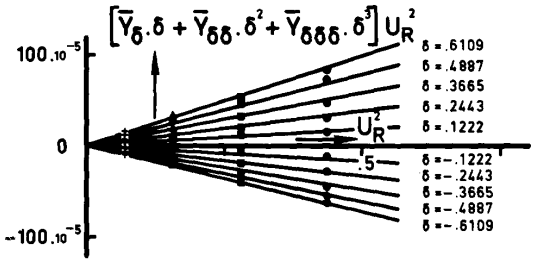

Figure 30 Lateral Force due to Rudder Deflection (Small Model 1:100)

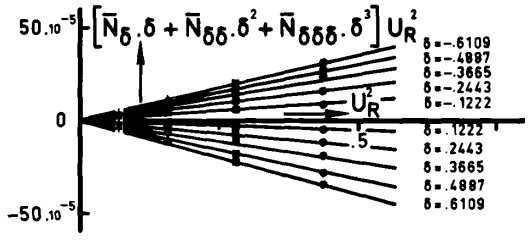

Figure 31 Lateral Moment due to Rudder Delection (Small Model 1:100)

SMALL MODEL 1:100

	●	■	▲	+
U_x (m/sec)	.80	.64	.48	.32
n (r.p.s.)	16.43	13.14	9.86	6.57

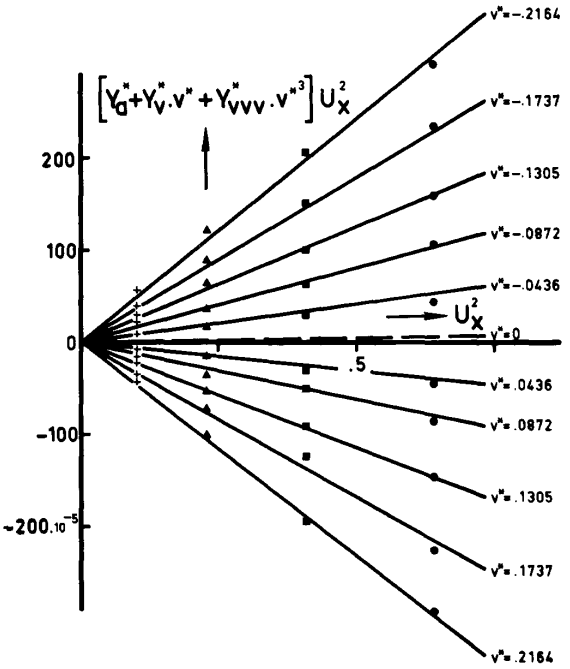

Figure 32 Lateral Sway Damping Force (Small Model 1:100)

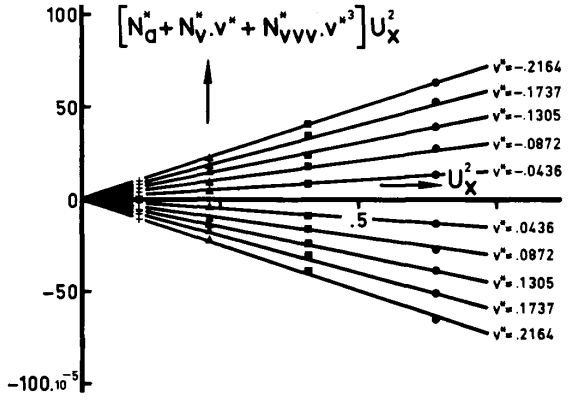

Figure 33 Lateral Sway Damping Moment (Small Model 1:100)

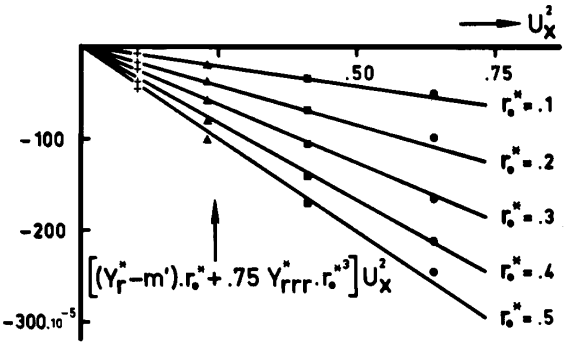

Figure 34 Lateral Yaw Damping Force (Small Model 1:100)

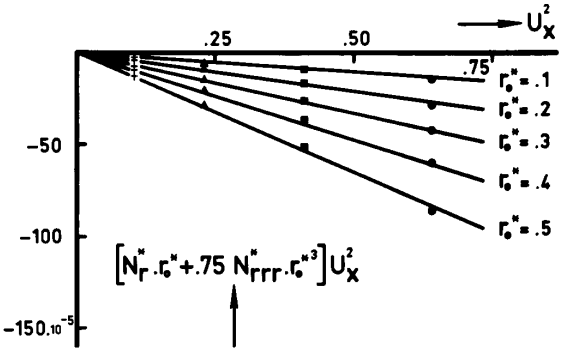

Figure 35 Lateral Yaw Damping Moment (Small Model 1:100)

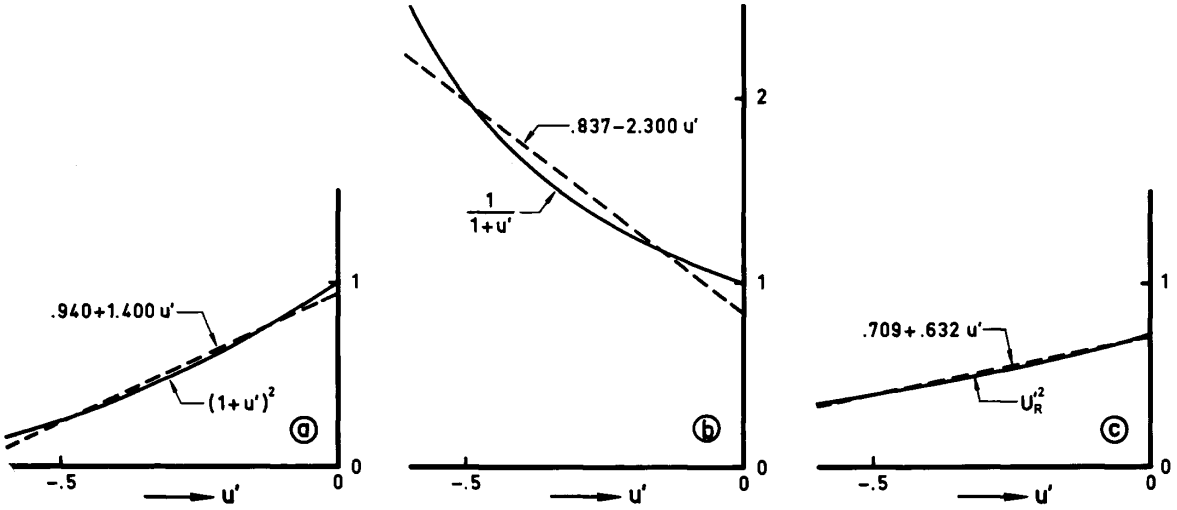

Figure 36 Some Linearisations

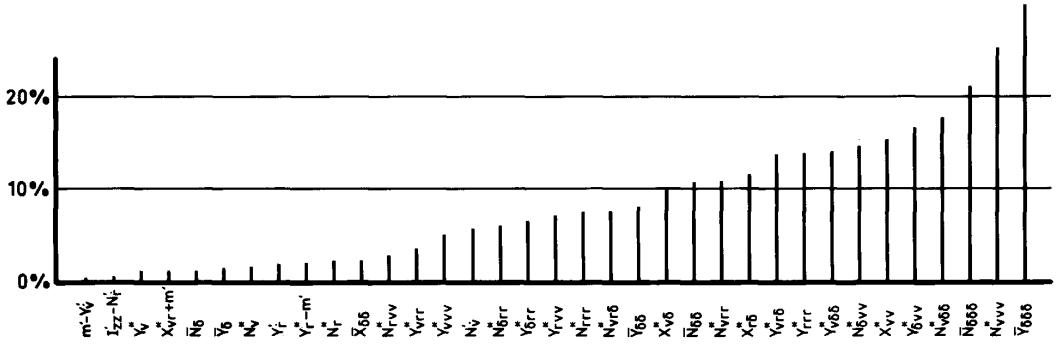

Figure 37 Standard Deviations of Coefficients

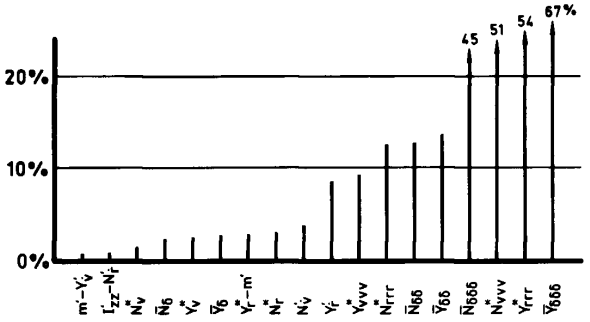

Figure 38 Standard Deviations of Coefficients (Small Model 1:100)

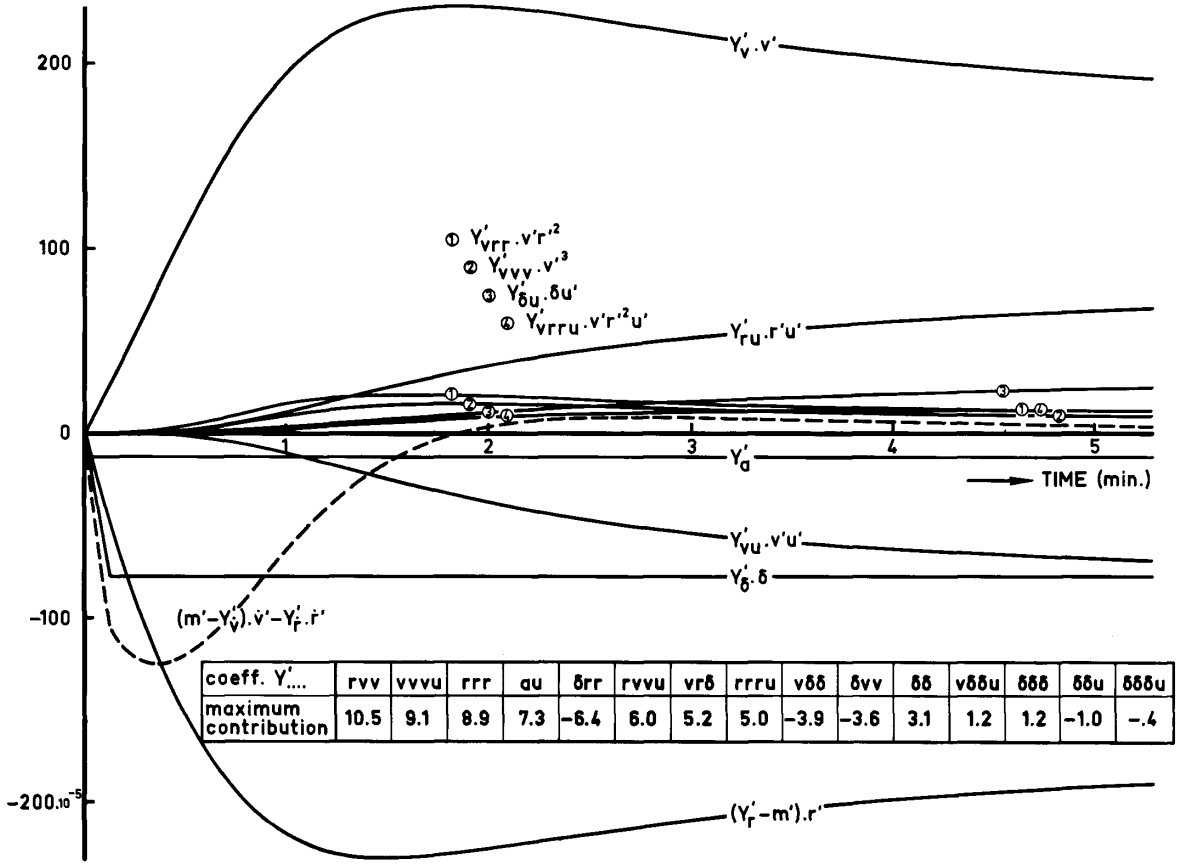

coeff. Y'....	rvv	vvvu	rrr	au	δrr	rvvu	vrδ	rrru	vδδ	δvv	δδ	vδδu	δδδ	δδu	δδδu
maximum contribution	10.5	9.1	8.9	7.3	-6.4	6.0	5.2	5.0	-3.9	-3.6	3.1	1.2	1.2	-1.0	-.4

Figure 39 Time Histories of Separate Terms in Side Force Equation of Turning Circle D2

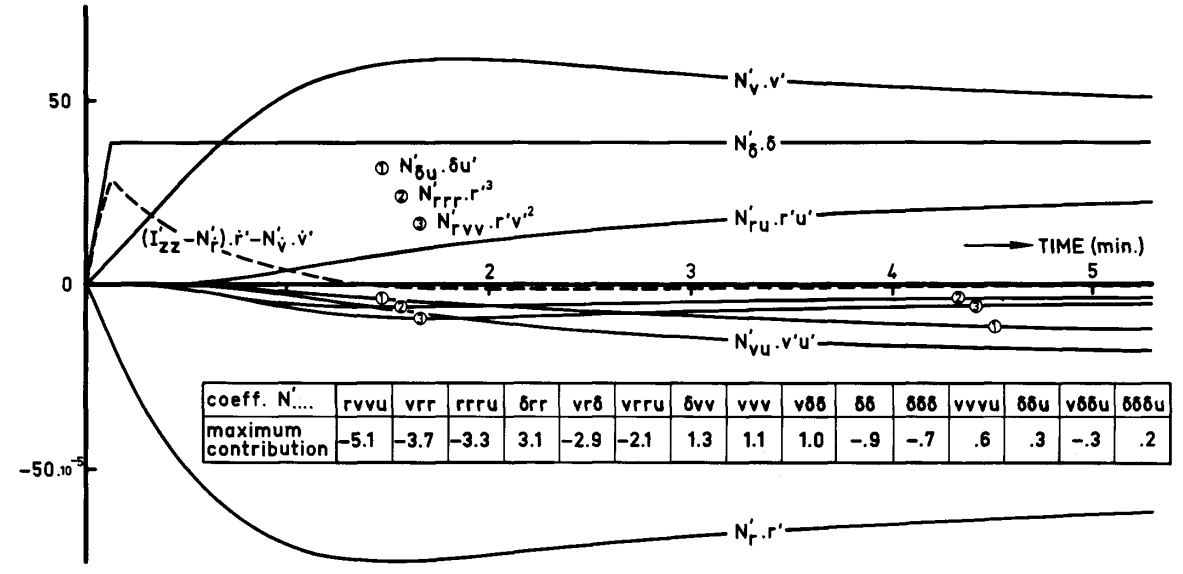

coeff. N'....	rvvu	vrr	rrru	δrr	vrδ	vrru	δvv	vvv	vδδ	δδ	δδδ	vvvu	δδu	vδδu	δδδu
maximum contribution	-5.1	-3.7	-3.3	3.1	-2.9	-2.1	1.3	1.1	1.0	-.9	-.7	.6	.3	-.3	.2

Figure 40 Time Histories of Separate Terms in Moment Equation of Turning Circle D2

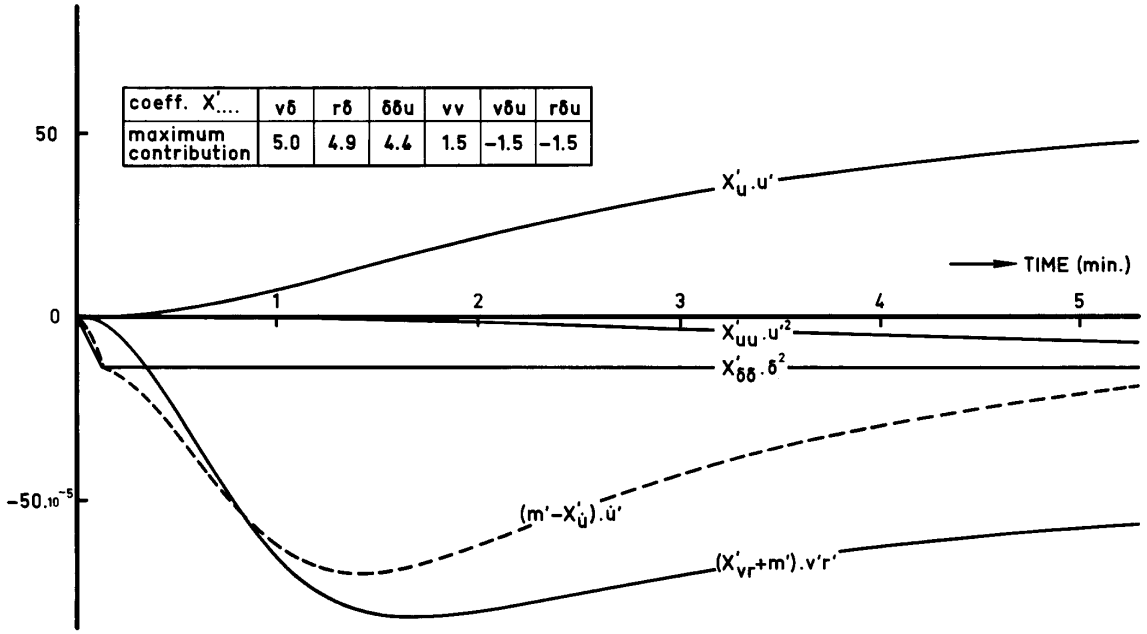

Figure 41 Time Histories of Separate Terms of Longitudinal Force Equation of Turning Circle D2

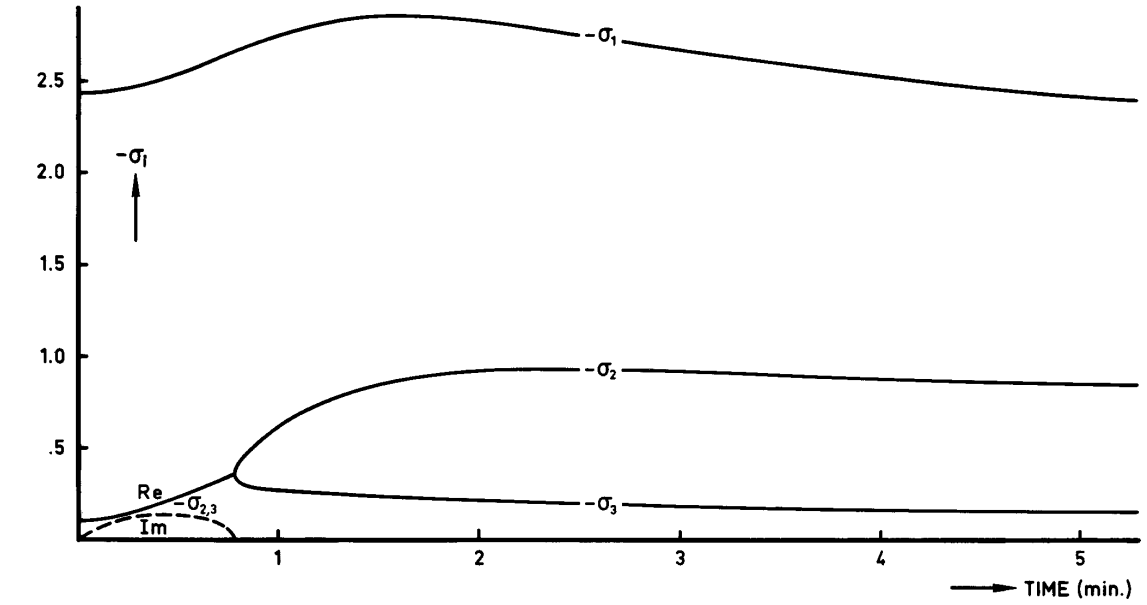

Figure 42 Time Histories of Stability Roots of Turning Circle D2

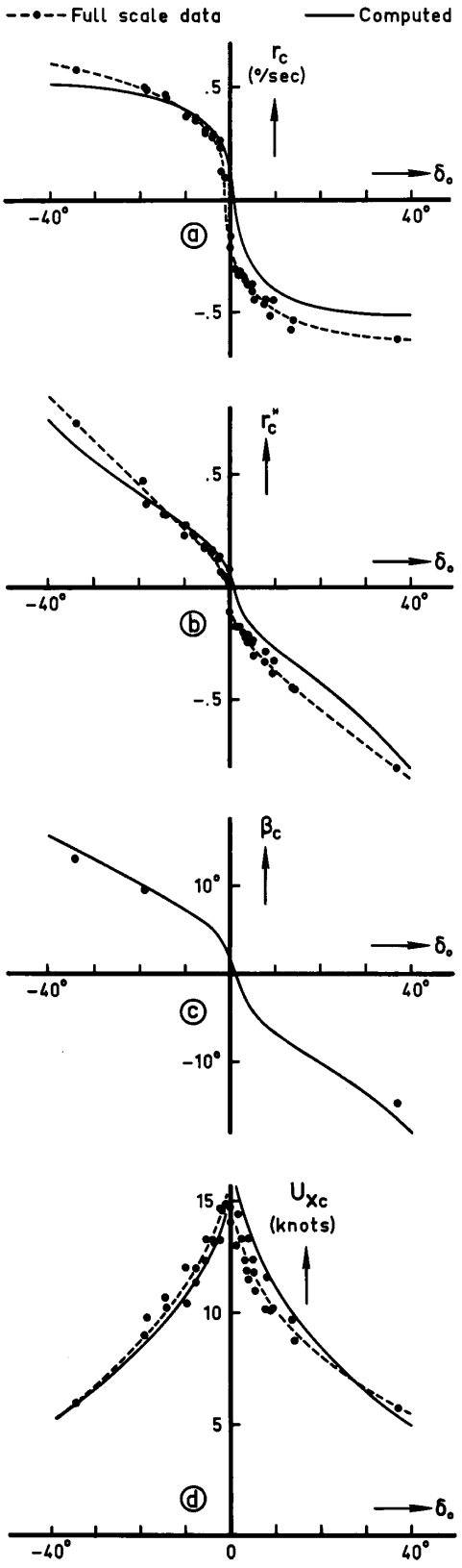

Figure 43 Turning Circle Characteristics at 100 Nominal RPM

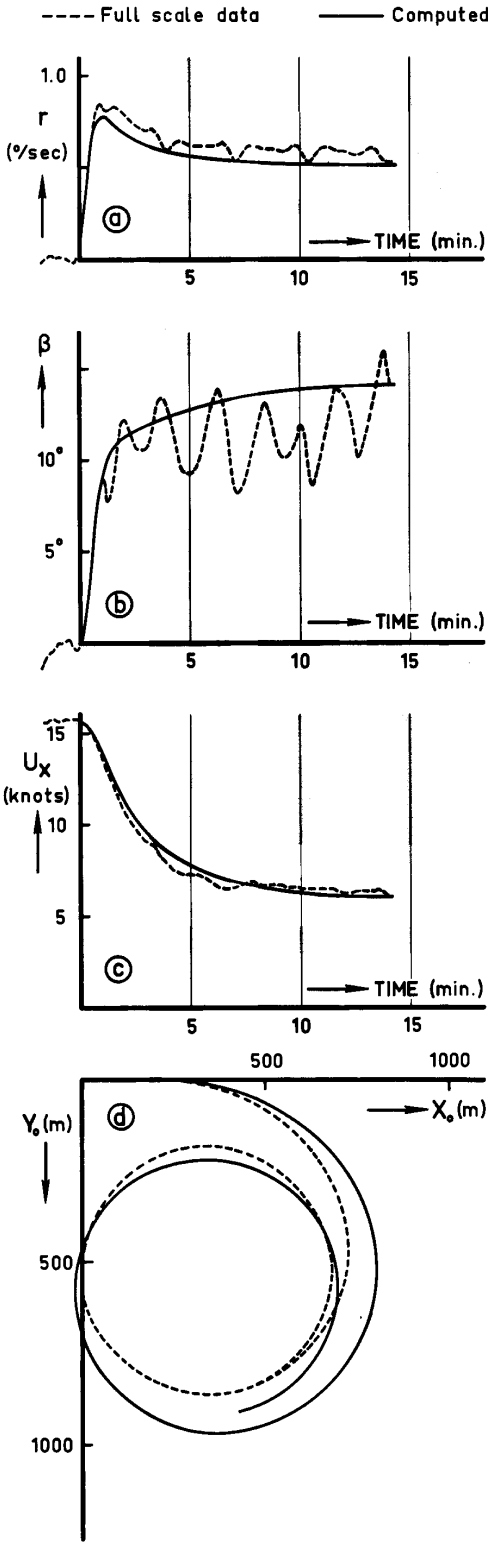

Figure 44 Time Histories and x-y Plot of Turning Circle A at 34^0 to Starboard and 100 Nominal RPM

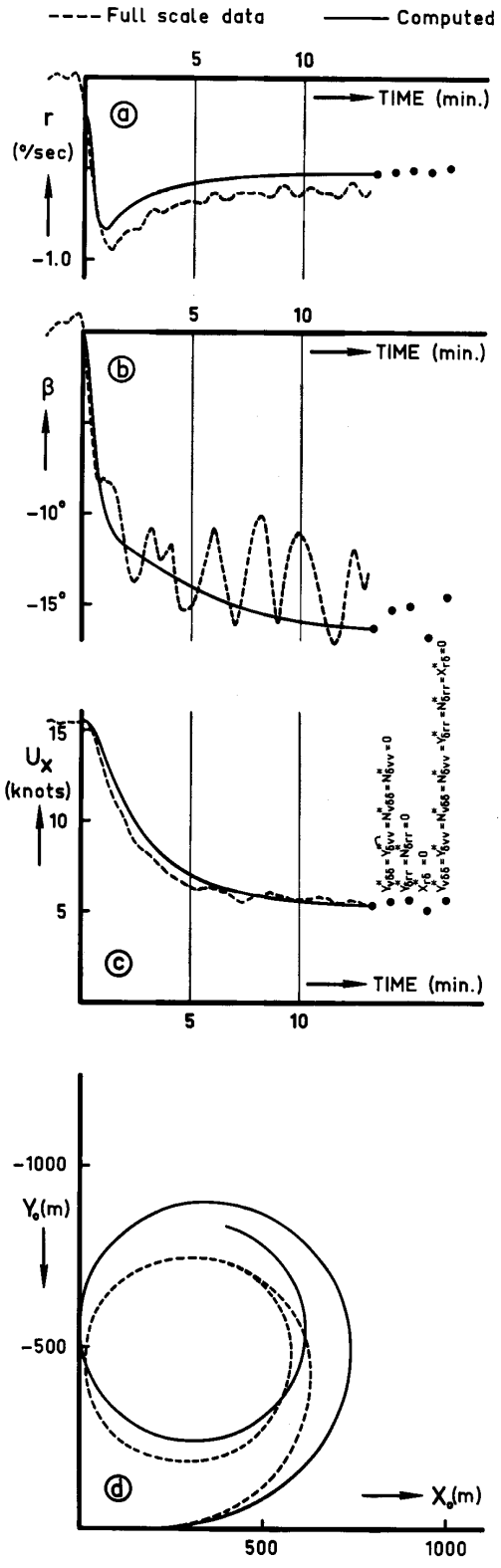

Figure 45 Time Histories and x-y Plot of Turning Circle B at 37^0 to Port and 100 Nominal RPM

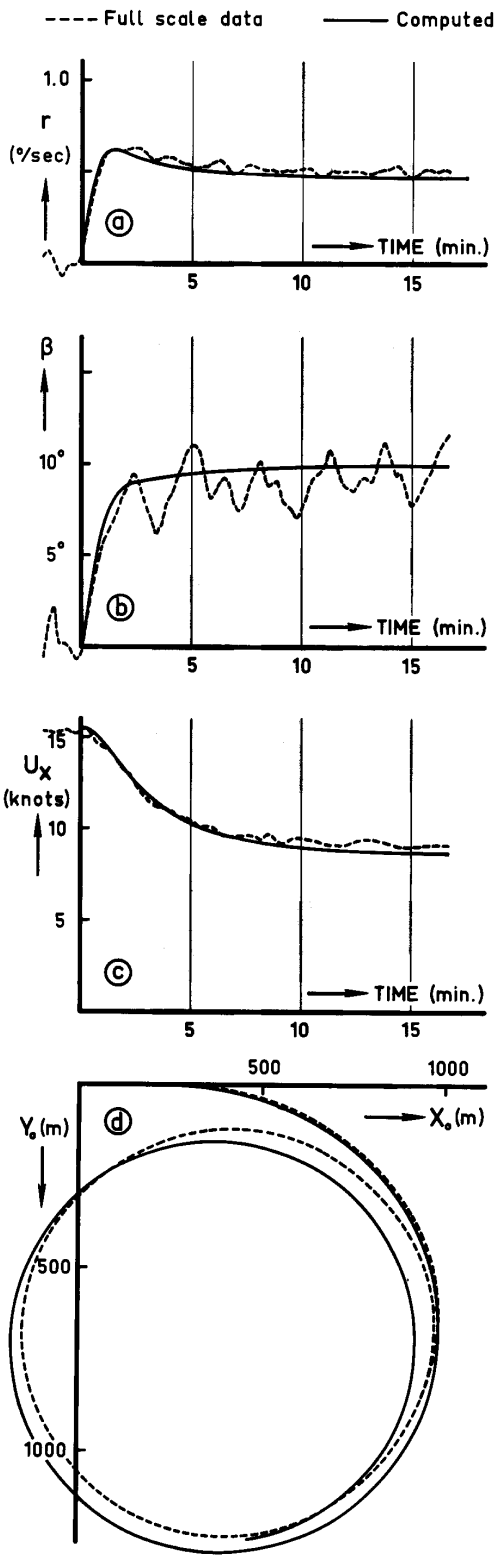

Figure 46 Time Histories and x-y Plot of Turning Circle D2 at 19^0 to Starboard and 100 Nominal RPM

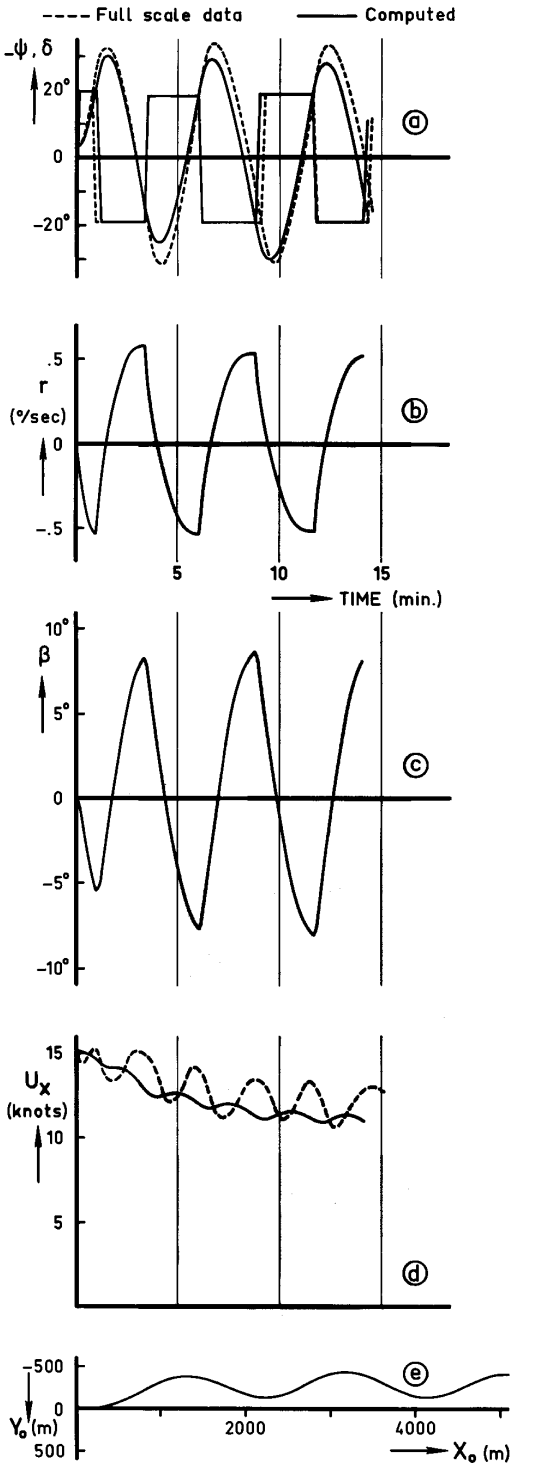

Figure 47 Time Histories and x-y Plot of Zig-Zag Test (20/20) at 100 Nominal RPM

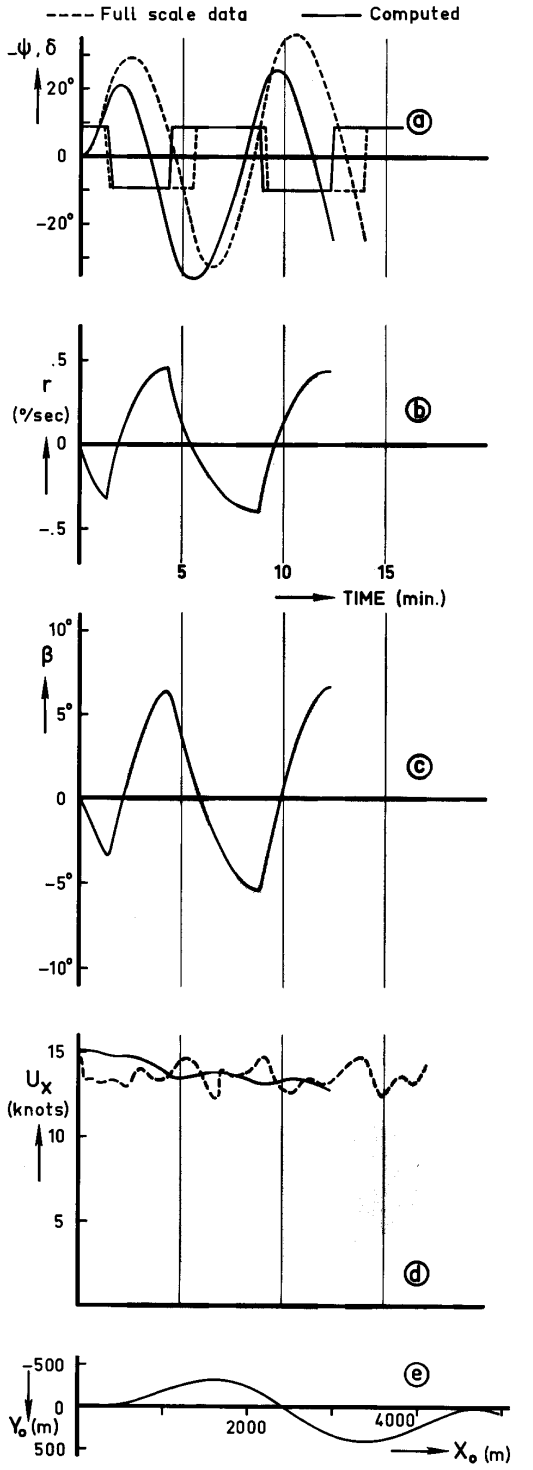

Figure 48 Time Histories and x-y Plot of Zig-Zag Test (10/20) at 100 Nominal RPM

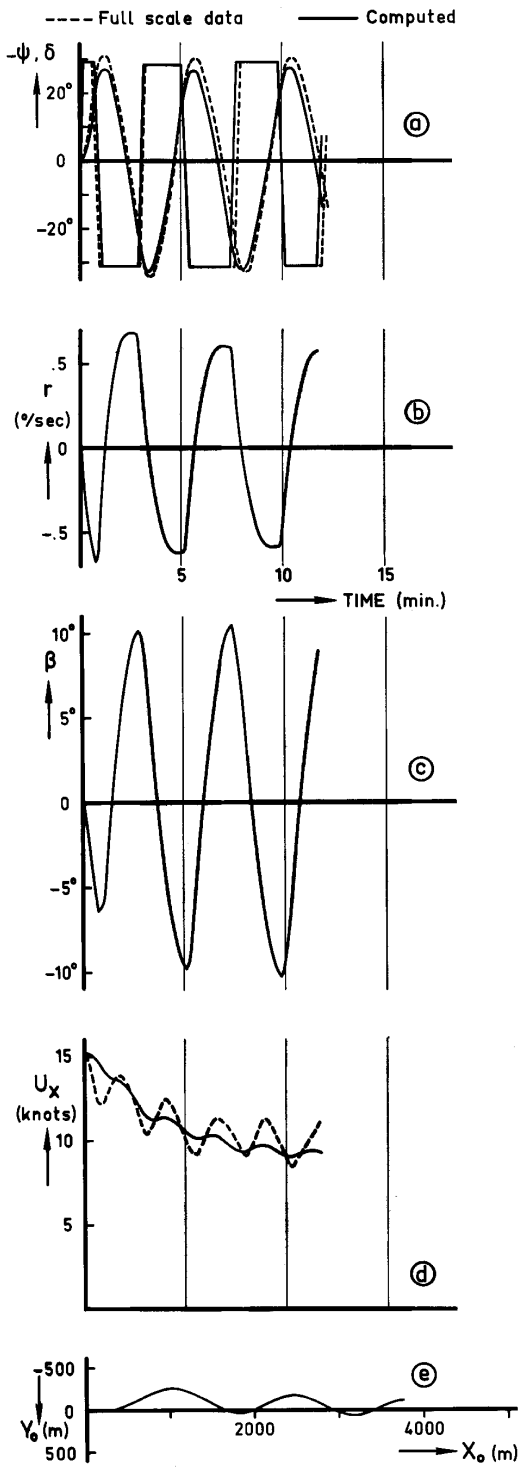

Figure 49 Time Histories and x-y Plot of Zig-Zag Test D (30/20) at 100 Nominal RPM

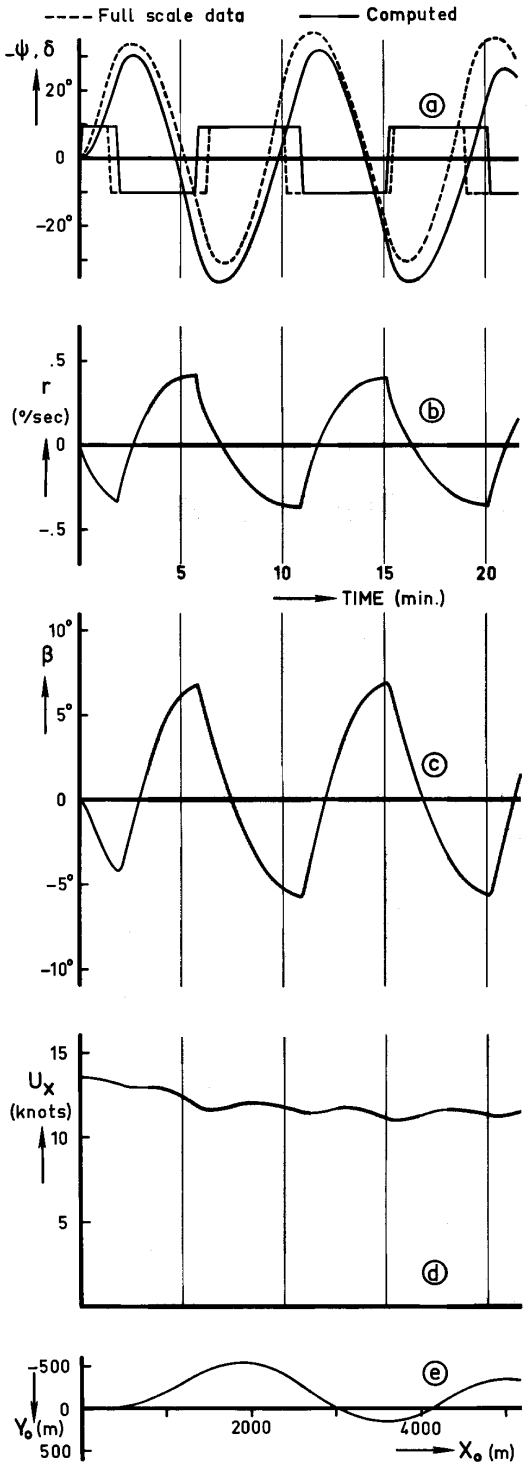

Figure 50 Time Histories and x-y Plot of Zig-Zag Test E (10/20) at 85 Nominal RPM

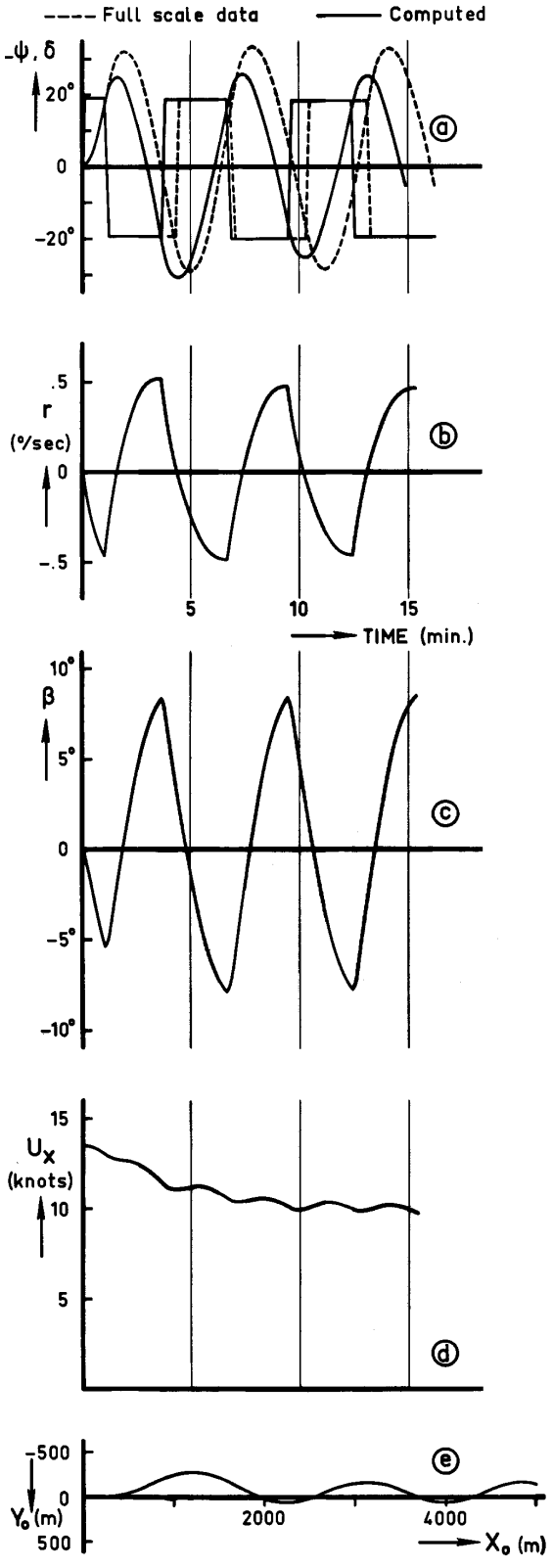

Figure 51 Time Histories and x-y Plot of Zig-Zag Test F (20/20) at 85 Nominal RPM

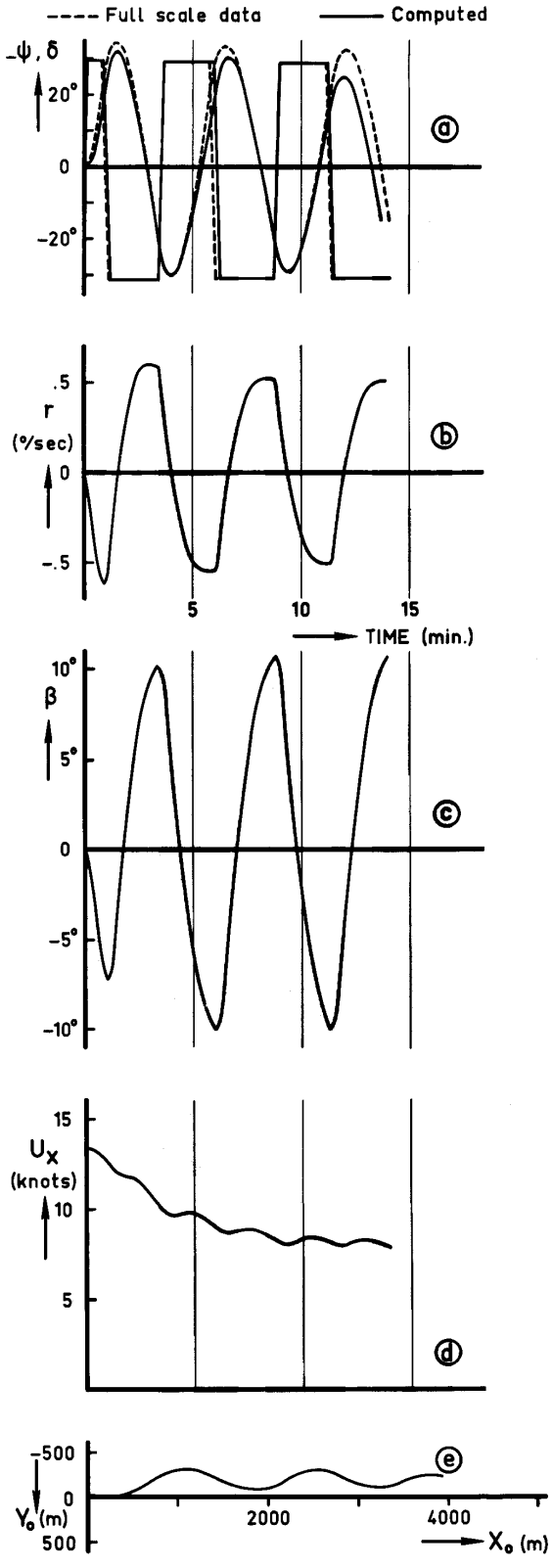

Figure 52 Time Histories and x-y Plot of Zig-Zag Test G (30/20) at 85 Nominal RPM

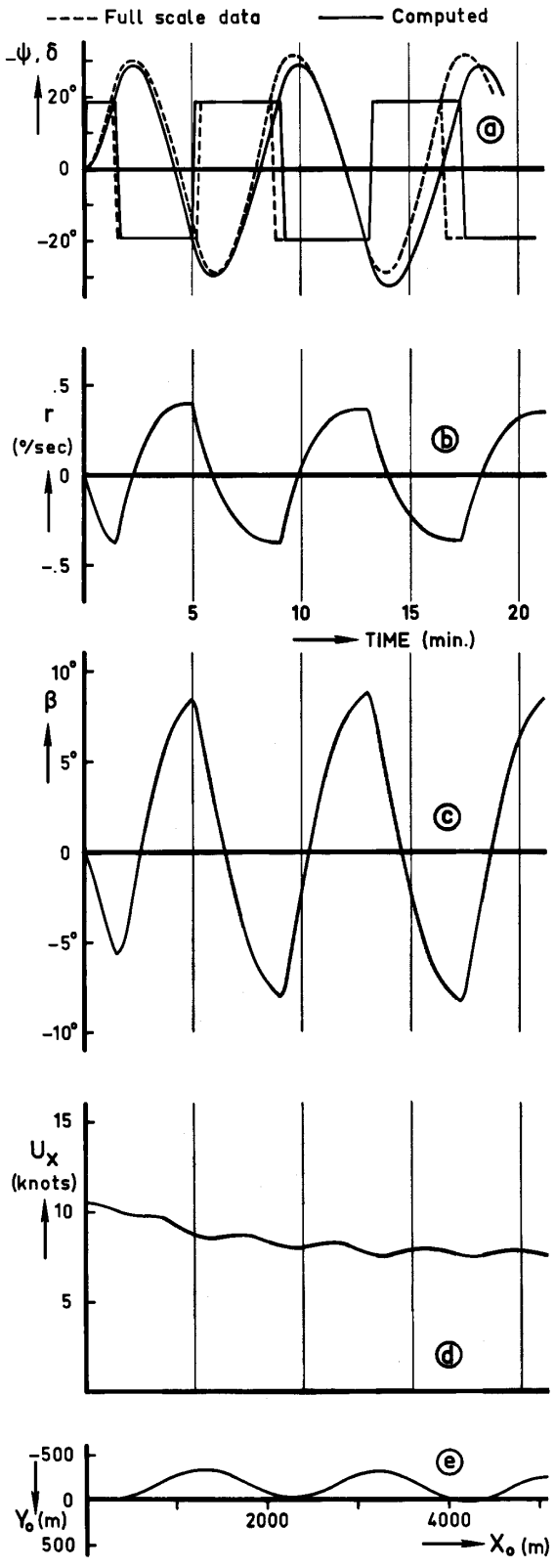

Figure 53 Time Histories and x-y Plot of Zig-Zag Test J (20/20) at 70 Nominal RPM

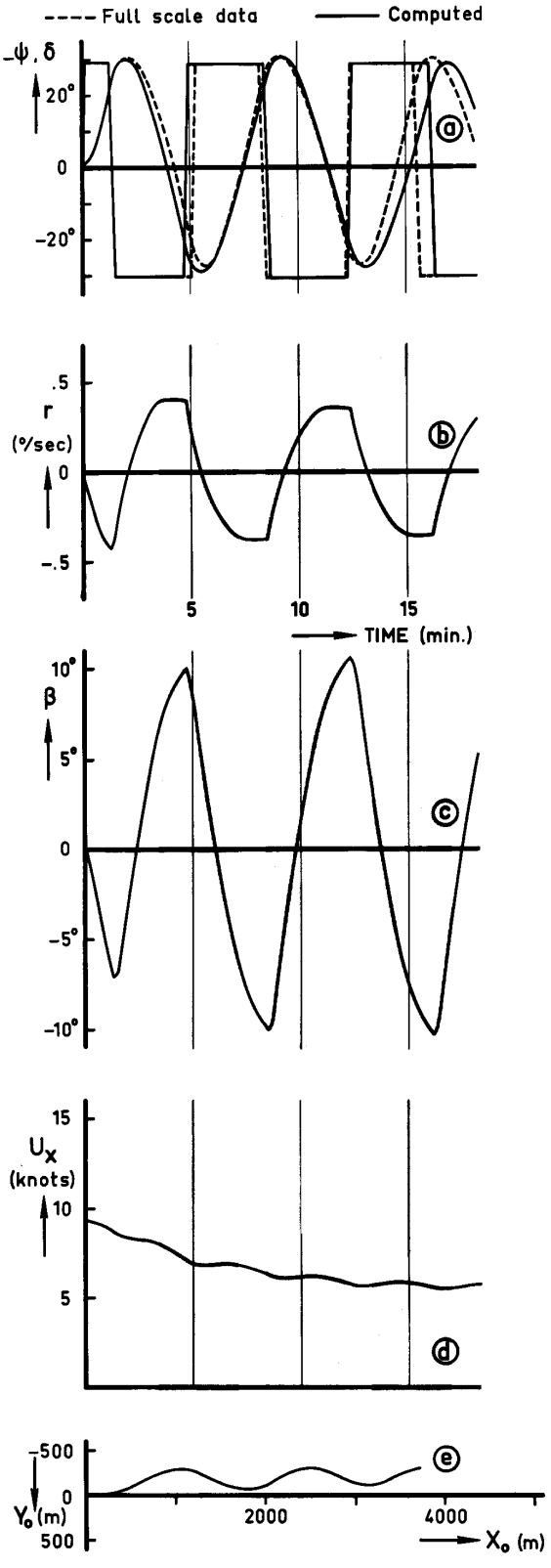

Figure 54 Time Histories and x-y Plot of Zig-zag Test L (30/20) at 60 Nominal RPM

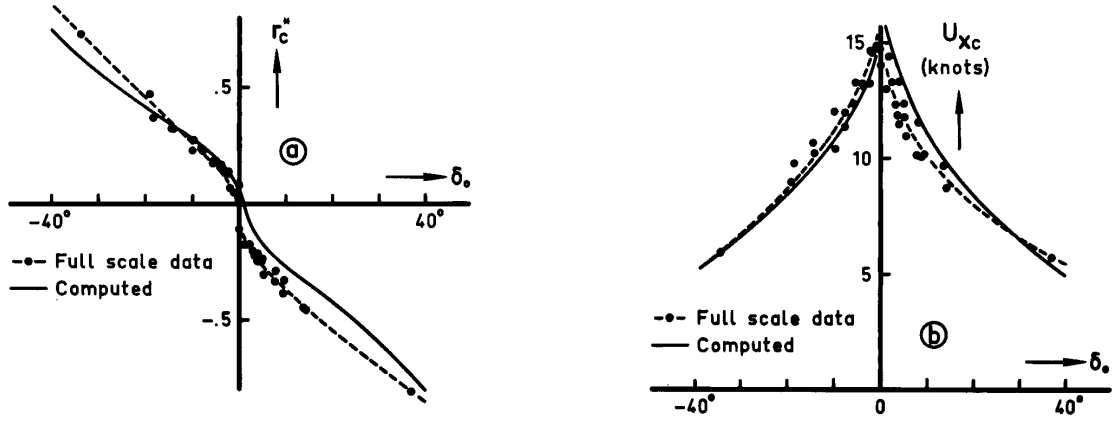

Figure 55 Principal Results of Predicted Turning Circles at 100 Nominal RPM

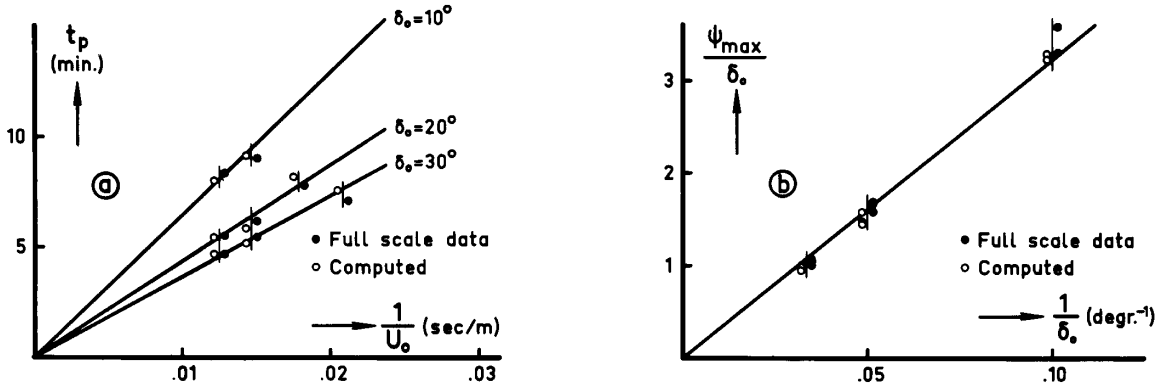

Figure 56 Principal Results of Predicted Zig-Zag Test